Chapter 25
Recent Advances in the Synthesis of Heterocycles Over Heterogeneous Cerium-Based Nanocatalysts

Cong Chien Truong, Dinesh Kumar Mishra, and Hoang Long Ngo

Contents

Abbreviations

$(NH_4)_2Ce(NO_3)_6$	Ceric ammonium nitrate
$(NH_4)_2CO_3$	Ammonium carbonate
Brij35	Polyoxyethylene (23) lauryl ether
$Ce(NO_3)_3.\ 6H_2O$	Cerium (III) nitrate hexahydrate
$CeCl_3$	Cerium (III) chloride
CeO_2/ceria	Cerium (IV) oxide

C. C. Truong (✉)
Department of Bio-functional Molecular Engineering, Graduate School of Science and Engineering, University of Toyama, Toyama, Japan

D. K. Mishra
Department of Chemical Engineering and Research Institute of Industrial Science (RIST), Hanyang University, Seoul, South Korea

H. L. Ngo
NTT Hi-Tech Institute, Nguyen Tat Thanh University, Ho Chi Minh City, Vietnam

A. Krishnan et al. (eds.), *Emerging Nanomaterials for Advanced Technologies*, Nanotechnology in the Life Sciences, https://doi.org/10.1007/978-3-030-80371-1_25

CH_3CN	Acetonitrile
CH_4	Methane
CO	Carbon monoxide
CO_2	Carbon dioxide
CTAB	Cetyltrimethylammonium bromide
$Cu(NO_3)_2$	Copper (II) nitrate
DMF	*N*,*N*-Dimethylformamide
DMSO	Dimethyl sulfoxide
$Eu(NO_3)_2$	Europium (III) nitrate
Luperox 101	2,5-Bis(*tert*-butylperoxy)-2,5-dimethylhexane
Lupersol TAEC	2-Ethylhexyl 2-methylbutan-2-yloxy carbonate
$Mg\ (NO_3)_2$	Magnesium (II) nitrate
MIL-101	Chromium terephthalate metal organic framework
NH_3	Ammonia solution
NO	Nitrogen (II) oxide
NPs	Nanoparticles
PEG 400	Polyethylene glycol 400
Pluronic 17R4	Poly(propylene glycol)-*block*-poly(ethylene glycol)-*block*-poly(propylene glycol)
Pluronic P123	Poly(ethylene glycol)-*block*-poly(propylene glycol)-*block*-poly(ethylene glycol)
PVA	Polyvinyl alcohol
PVP	Polyvinylpyrrolidone
$Zr(NO_3)_2$	Zirconium (II) nitrate

25.1 Introduction

Heterocycle is an important class of compounds in organic chemistry, which can be found in wide applications from natural to man-made products. In nature, numerous heterocyclic skeletons can be found in plant/marine metabolites, chlorophyll, genetic building blocks, vitamins, essential oils, enzymes and so on (Walsh 2015). Alternatively, novel synthetic compounds containing various heteroatoms and/or fused ring systems have been successfully constructed over the years (Taylor et al. 2016). For the assembly of complex molecules, these privileged structures turned out to be versatile and valuable building blocks in the synthesis of natural products (Carson and Kerr 2009; Majumdar and Chattopadhyay 2011), organic semiconductors (Zhao et al. 2017), high-density energy materials (Yin and Shreeve 2017), agrochemicals (Lamberth 2013), polymers (Lu 1998), etc. Due to the diverseness in architectural complexity, molecular functionality and bioactivity, the exploration of heterocycles is considered of great significance in medicinal chemistry (Fig. 25.1) (Gomtsyan 2012). For instance, the US FDA databases show that 59% of small-molecule drugs are composed of *N*-heterocyclic fragments (Vitaku et al. 2014). In addition, other top-selling heterocyclic pharmaceuticals are currently exploited as

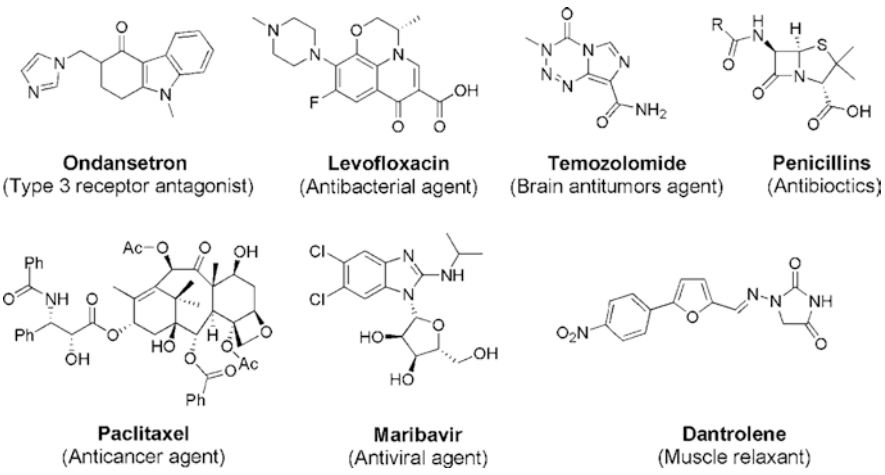

Fig. 25.1 Heterocyclic pharmaceuticals

anticancer, antibiotic, antiviral, antibacterial, diuretic and antineoplastic agents (Baumann et al. 2011; Baumann and Baxendale 2013; Ali et al. 2015; Feng et al. 2016; Delost et al. 2018). From these reasons, seeking simple but effective processes for the eco-friendly production of heterocycles has been considered as formidable challenges in both academia and industry throughout the years.

Recently, nanocatalysts have been widely acknowledged as powerful tools in the domain of heterogeneous catalysis, where nanostructured metal oxides and their hybrid materials attracted significant attention due to their superb catalytic efficiency in many chemical transformations (Wang et al. 2009; Guo et al. 2014; Gadipelly and Mannepalli 2019). In this manner, simple preparation, excellent thermal/chemical stability, high surface area, tunable control of acidity/basicity, low cost and recyclability are conducive to their versatility. Among the rare earth metal-based nanoparticles, most of the researches focused on the application of cerium-based materials as both catalyst and support due to the abundant, unique and tunable features of cerium (Sun et al. 2012; Zhang et al. 2012; Paier et al. 2013; Huang and Gao 2014). For example, the oxygen vacancies and reversible valence change (Ce^{4+} and Ce^{3+}) in CeO_2 allowed this nanostructure to participate in copious reactions such as oxidation, hydrogenation, methane reforming, water-gas shift, CO_2 conversion and others (Chang et al. 2019; Rodriguez et al. 2017). Moreover, the outstanding catalytic performance of ceria-supported transitional metals (e.g., Pd, Pt, Rh and Au), cerium mixed oxides, or cerium-doped solid materials in CH_4/CO/NO oxidation (Cargnello et al. 2012; Colussi et al. 2009; Spezzati et al. 2017; Qi and Li 2015), ozonation (Orge et al. 2012; Xu et al. 2016), hydrogenation (Akbayrak 2018; Hu et al. 2018) and photochemical reactions (Channei et al. 2014; Fiorenza et al. 2016; Shi et al. 2011) was also realized. Prompted by aforementioned reasons, several research groups have recently turned their keen eyes on the utility of cerium-based solids in organic chemistry (Vivier and Duprez 2010; Naaz et al. 2019), where

the acid/base, redox or dual (acid/base-redox) sites on these heterogeneous catalysts served the crucial roles in determining the activity. To the best of our knowledge, a holistic overview on the practicality of cerium-based nanocatalysts in the construction and functionalization of heterocycles has not been reported. In this book chapter, numerous examples on the green and sustainable assembly of heterocyclic frameworks over well-defined cerium oxide/mixed oxides, cerium composites, cerium-doped solids and ceria-supported metals are introduced. In particular, the deployment of nanoceria in the chemical fixation of CO_2 towards valuable cyclic products is also explored. Furthermore, mechanistic description on each transformation is discussed in detail to give further insight on the activity of cerium-based nanocatalyst.

25.2 Applications of Cerium-Based Catalysts in the Synthesis and Functionalization of Heterocycles

25.2.1 Commercial CeO_2

In 2014, Edayadulla and Lee (2014) explored the catalysis of commercial CeO_2 NPs in the divergent synthesis of quinoxalin-2-amines and 3,4-dihydroquinoxalin-2-amines. By using 5 mol% of CeO_2, the one-pot condensation of 1,2-diamines, isocyanides with aldehydes or ketones could undergo smoothly in water to render a multiple of quinoxalin-2-amine and 3,4-dihydroquinoxalin-2-amine derivatives, respectively. Furthermore, the utility of CeO_2 NPs was also successfully attempted in the construction of indophenazine derivatives from the coupling of 1,2-phenylenediamine, isatins with *tert*-butyl isocyanide. The model mechanistic concourse towards quinoxalin-2-amine starting from 1,2-phenylenediamine, aldehyde and isocyanide is described to follow a cascade of imine formation/addition of isocyanide/annulation/isomerization/oxidation (Scheme 25.1), where CeO_2 NPs are demonstrated to facilitate the generation of imine and the insertion of isocyanide into imine.

Later, Shrestha et al. (2016) expanded the utility of CeO_2 NPs for the eco-friendly assembly of spiro[indoline-3,4-pyrano[2,3-*c*]pyrazole] derivatives. Under assistance of 30 mol% of CeO_2, a plenty of fused spirooxindoles could be afforded in the range yields of 75–93% from the aqueous-phase condensation of β-ketoesters with phenylhydrazines, malononitrile and isatins (Scheme 25.2). Particularly, a number of designed spirooxindole derivatives showed promising results on the potent antioxidant and antibacterial activities.

In another case, Sharma et al. (2018) established a novel synthetic strategy for fused tetrahydroisoquinolines and pyrrolo[3,4-c]quinoline-1,3-diones by coupling *N*,*N*-dimethylanilines **1** with *N*-substituted maleimides **2** over CeO_2 NPs. As shown in Scheme 25.3, tetrahydroisoquinoline derivatives with a high tolerance of functionality were obtainable upon performing the oxidative annulation of **1** and **2** with

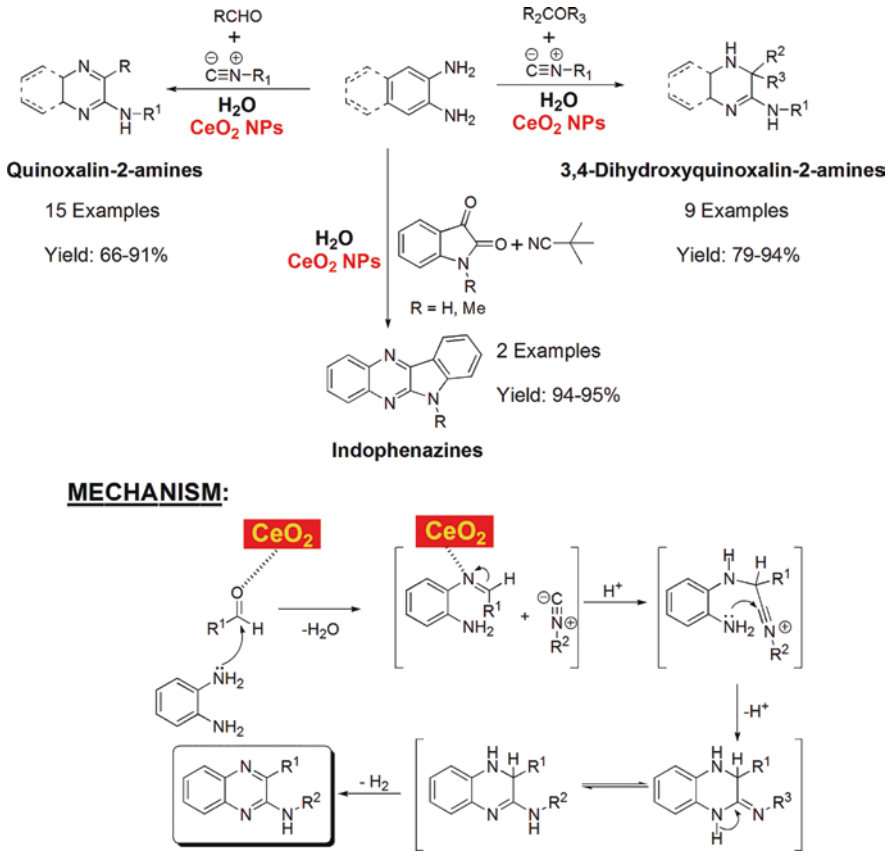

Scheme 25.1 Divergent synthesis of quinoxalin-2-amines, 3,4-dihydroquinoxalin-2-amines and indophenazines over CeO_2 NPs

20% mol of CeO_2 in air under optimal conditions. Afterwards, these resulting tetrahydroisoquinolines were efficiently transformed into quinoline-1,3-diones through the dehydrogenative/*N*-demethylative cascade in the presence of 2,3-dichloro-5,6-dicyano-1,4-benzoquinone (DDQ). Unluckily, the activity of recovered CeO_2 NPs was found to gradually drop after four recycles. In the mechanistic proposal, the model assembly of pyrrolo[3,4-c]quinoline-1,3-diones is proposed to follow the sequential stage of oxidative annulation/dehydrogenation/*N*-demethylation.

Besides, CeO_2 was also exploited as a robust catalyst in functionalizing the heterocyclic skeletons. For example, CeO_2 NPs was effective in promoting the aerobic cross-dehydrogenative coupling (CDC) of *N*-aryl tetrahydroisoquinolines with either nitroalkanes or acetone, which delivered a collection of corresponding 1-sub stituted-2-aryl-1,2,3,4-tetrahydroisoquinoline derivatives (Sharma et al. 2016a). Through a set of control experiments, the model mechanism for the oxidative CDC of *N*-phenyl tetrahydroisoquinoline and nitromethane via radical pathway is

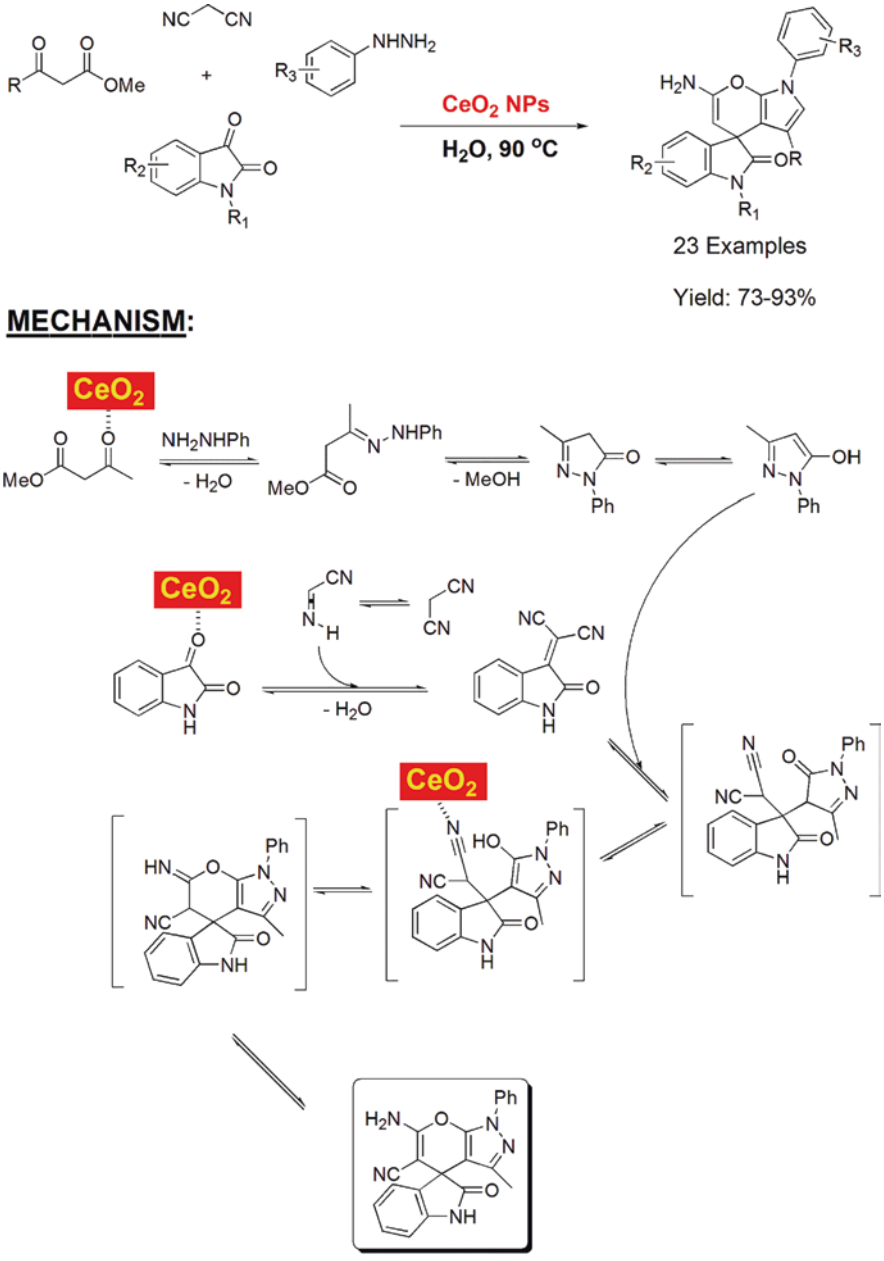

Scheme 25.2 CeO_2-mediated assembly of spiro[indoline-3,4-pyrano[2,3-*c*]pyrazole] derivatives in water

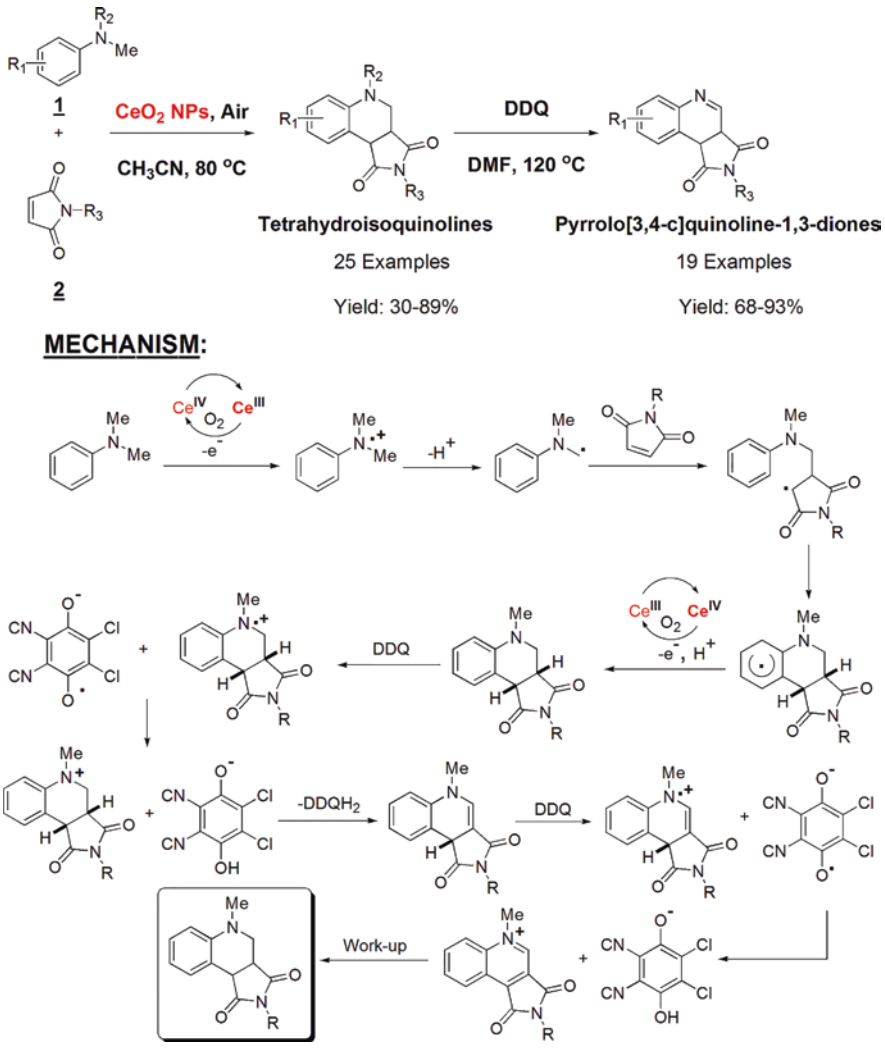

Scheme 25.3 Synthesis of tetrahydroisoquinolines and pyrrolo[3,4-c]quinoline-1,3-diones from the CeO_2/DDQ-mediated coupling of *N*,*N*-dimethylanilines and *N*-substituted maleimides

established in Scheme 25.4. In this context, Ce^{4+} would be transformed into Ce^{3+} and vice versa in the presence of O_2 during the single-electron transfer (SET) to facilitate the formation of iminium intermediate. Significantly, only a minor diminution in the yields of *N*-aryl tetrahydroisoquinoline was observed after four circulations of spent CeO_2.

In addition, Rashed et al. (2020) demonstrated that the commercial CeO_2 (JRC-CEO-1, 185.3 m^2/g) could stimulate the solvent-free alkenylation of oxindole with aldehydes (Scheme 25.5). Specifically, this synthetic protocol was applicable to

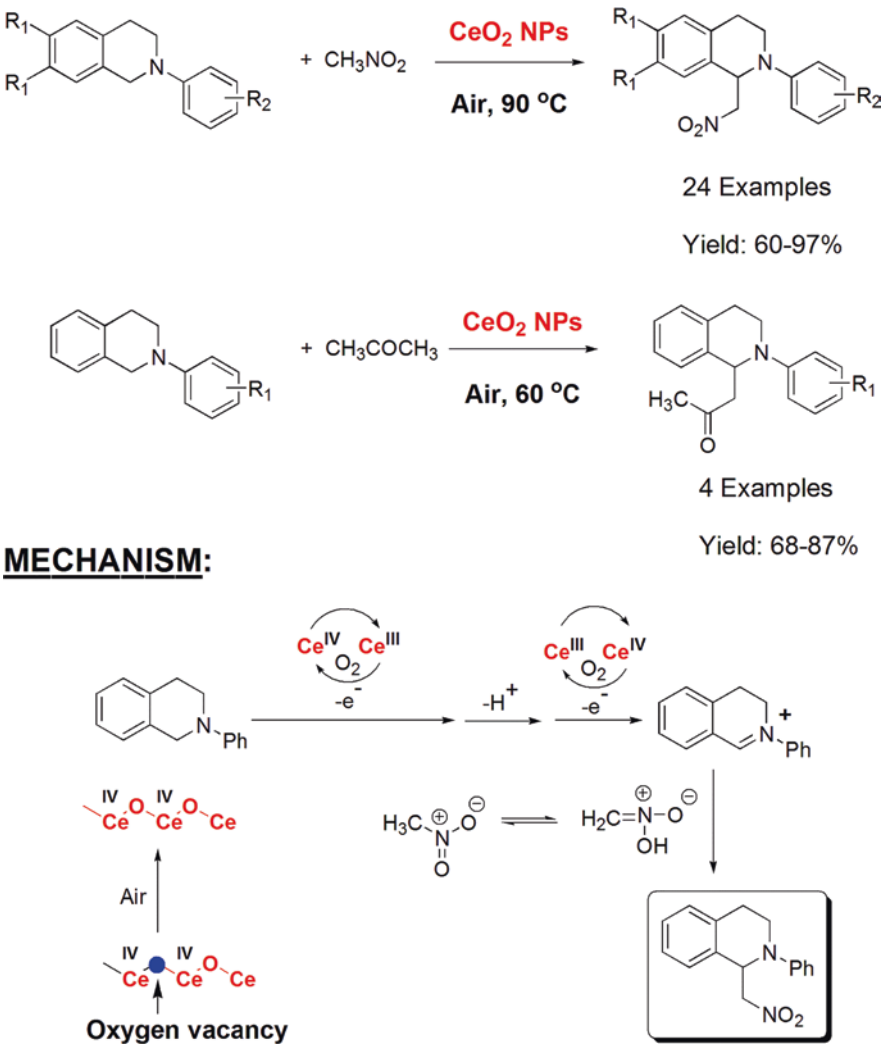

Scheme 25.4 Functionalization of *N*-aryltetrahydroisoquinolines with nitroalkanes and acetone over nanostructured CeO_2

both aliphatic and aromatic aldehydes, furnishing 87–99% yields of C_3-alkenylated oxindole products with high selectivity in *E* isomers. In this study, a close relationship between catalytic activity and morphology of CeO_2 calcined at different temperatures (i.e. 300, 500, 600, 800 and 1000 °C) was described. Surprisingly, the ceria with increasing calcination temperature would display higher catalytic activity despite their lower specific area, which might be attributed to the presence of non-defect (111) surface as active sites for the alkenylation reaction. Another reason came from the assumption that elevating the calcination temperature in the

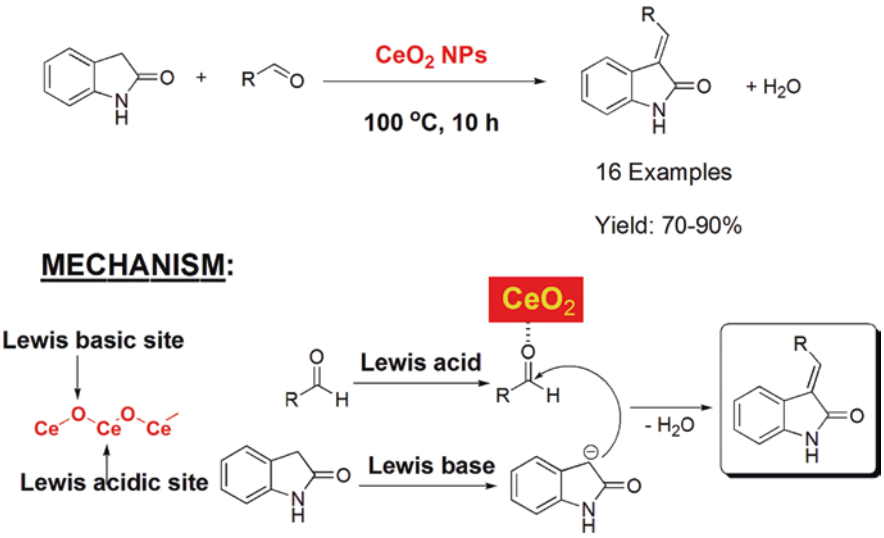

Scheme 25.5 C_3-alkenylation of oxindole with aldehydes towards 3-alkyledene oxindoles over CeO_2 NPs

pretreatment stage led to a higher density of Lewis active sites. Indeed, the outstanding catalytic activity of nanostructured CeO_2 in this alkenylation was accredited to the bifunctional Lewis acid-base property, in which the basic sites (oxygen atom) would deprotonate the C_α-H bond of oxindole to trigger the corresponding enolate ion. Meanwhile, the acidic sites (cerium atom) would activate the carbonyl group of aldehyde, thereby enhancing the reactivity of C=O bond towards the nucleophilic attack of enolate.

25.2.2 Synthetic Nano-CeO_2

In nanotechnology, a plethora of techniques have been developed to fabricate the metal oxide nanoparticles (Table 25.1) (Rane et al. 2018). With each type of synthetic mode, the nanostructured oxides with different physical-chemical properties (e.g. particle size, porosity, defect, crystal structure, polarity and acidity/basicity) can be selectively controlled. In this regard, the reaction conditions such as starting precursors, capping agents, pH, ageing time/temperature and calcination temperature are key factors governing the outcome of final nanostructures. For instance, copious exemplars showing the impact of synthetic procedures on the specific morphology of CeO_2 NPs are illustrated in Table 25.2.

In this chapter, all of the reported nanostructured CeO_2 could be prepared from four main synthetic categories of co-precipitation, template, biological and sol-gel pattern.

Table 25.1 Synthetic techniques of nanoparticles

Synthetic modes of nanoparticles			
Co-precipitation synthesis	Sol-gel synthesis	Ultrasound synthesis	Laser ablation synthesis
Hydrothermal synthesis	Template synthesis	Microwave-assisted synthesis	Sputtering synthesis
Inert gas condensation synthesis	Microemulsion synthesis	Spark discharge synthesis	Biological synthesis

Table 25.2 Impact of synthetic methods on the morphology of CeO_2

Method	Cerium precursor	Capping agent	Particle size (nm)	Morphology	References
Precipitation	Cerium (III) nitrate	–	9–18	Cubic hexagonal	Chen and Chen (1993)
		PVP	27	Spherical	
Microemulsion	Cerium (III) nitrate	Hexamethylenetetramine	7–10	Spherical	Arya et al. (2014)
	Cerium (III) nitrate-Cerium (III) chloride	Brij35	6–13	Cubic	Bumajdad et al. (2004)
Hydrothermal	Cerium (III) nitrate	–	8–16	Cubes, rods	Arya et al. (2014)
	Cerium (III) chloride	Citric acid	<5	Spherical	López et al. (2015)
Biological	Cerium (III) nitrate	*Hibiscus sabdariffa*	3.9	Amorphous	Thovhogi et al. (2015)
	Cerium (IV) ammonium nitrate	Fructose/glucose/lactose	2–6	Spherical/ agglomerate	Kargar et al. (2015)
Sol-gel	Cerium (III) nitrate	Oleylamine	1.2–35	Spherical, tadpole, wire	Yu et al. (2005)

Co-precipitation (Guo et al. 2015) This is the most facile and convenient strategy to fabricate metal oxide nanoparticles by adding a precipitating agent (organic or inorganic bases) into the aqueous solution of metal salts at room or elevated temperature. As soon as the concentration of species present in the solution reaches the critical point, a cascade of nucleation/growth/agglomeration reaction will take place. In some cases, employing the surfactants and capping agents is necessary to selectively manipulate the physiochemical and catalytic features of the final metal oxides. Undoubtedly, multiple factors such as precursors, nature of bases, pH of the reaction medium, temperature, and stirring rates strongly influence the property of designed metal nanoparticles. For instance, Chen and Chang (2005) disclosed that increasing the temperature in the co-precipitation of $Ce(NO_3)_3.6H_2O$ with NH_3 led to a morphological change of CeO_2 particles from cubic to hexagonal, whilst lower-

ing the temperature induced the smaller size of ceria particles. On the other hand, the elevation of pH towards 12 in the reaction medium helped to decrease the crystallite size of CeO_2 (Ramachandran et al. 2019). Other influential factors in the co-precipitation for CeO_2 such as cerium precursors and precipitating agents are illustrated in the Table 25.3 as well. In fact, rapid, safe, low-cost, facile and organic solvent-free aspects are acknowledged as remarkable merits of this synthetic strategy.

Sol-gel synthesis (Parashar et al. 2020; Laberty-Robert et al. 2006) This model is associated with the rapid hydrolysis of metal-organic precursors in water and/or organic solvents to generate the corresponding metal oxo-hydroxides, which subsequently undergo the condensation to form an extended matrix of metal hydroxides. Next, the polymerization of these hydroxides will lead to the establishment of a dense network porous gel. Afterwards, the ultrafine porous metal oxides can be obtained upon drying and heating the gel at high temperatures. In this situation, the nature of both metal precursors and solvents considerably determines the morphology and particle size of final metal oxides. As an example, Yu et al. (2005) revealed that spherical CeO_2 could be triggered from the sol-gel treatment of $Ce(NO_3)_3.6H_2O$, diphenyl ether with oleylamine. On the other hand, the addition of oleic acid in this mixture resulted in wired or tadpole-like CeO_2 regarding to the amount of oleic acid. More examples on the sol-gel approach towards different CeO_2 NPs are depicted in Table 25.4.

Template-assisted synthesis (Yu et al. 2013) This technique mainly concerns with the deployment of hard/soft materials (e.g. carbon nanotube, alumina, zeolites, silica and polymers) as a host, where the nanoparticles will be fabricated and confined within the pores or channels of the template after calcination. By applying a proper choice of starting precursors, loading amounts and type of templates, it is able to render controlled-sized nanostructures with various morphologies (Table 25.5).

Table 25.3 Different types of nano-CeO_2 obtained from the co-precipitation

Cerium precursor	Precipitating agents	Particle size (nm)	Morphology	References
Cerium (III) nitrate	Ammoniac-ammonium bicarbonate	120–460	Spherical	Zhang et al. (2009)
	Sodium hydroxide	5	Rod	Du et al. (2007)
	Ammonia-hydrogen peroxide-hexamethylenetetramine	6	Cubic	Kamruddin et al. (2004)
Cerium (IV) ammonium nitrate	Urea	~8	Cubic	Tsai (2004)

Table 25.4 Different types of nano-CeO_2 obtained from the sol-gel strategy

Cerium Precursor	Medium	Particle size (nm)	Morphology	References
Cerium (IV) nitrate	Oleylamine-trioctylamine-diphenyl ether	1.2–3.5	Spherical, tadpole, wire	Yu et al. (2005)
Cerium (III) salts	PVA-sucrose	6–9	Cubic	Soni and Biswas (2013)
Cerium (IV) ammonium nitrate	CTAB-methanol-aniline	3.4–10.4	Sponge-like	Tillirou and Theocharis (2008)

Table 25.5 Different types of nano-CeO_2 from the template-directed synthetic pattern

Cerium precursor	Template	Particle size (nm)	Morphology	References
Cerium (III) nitrate	Carbon spheres	300	Hollow spherical	Xu et al. (2014)
Ammonium cerium (IV) nitrate	Polymethyl methacrylate	5	Tubular	Schneider et al. (2011)
Cerium (III) nitrate	Chitosan	~4	Cubic	Sifontes et al. (2011)

Biological synthesis (Malik et al. 2017) This synthetic mode involves the application of biological materials such as microorganisms (e.g. bacteria, fungi, yeast and algae), plant parts (e.g. leaves, fruit, flower, bark and seed) or sugars as natural reducing agents to assist the fabrication of nanoparticles. In the presence of these biochemical reductants, the metal ions from precursor salts are initially reduced to atoms which subsequently nucleate into small clusters. Originating from these metal clusters, the nanoparticles will grow in different manners depending on the concentration of metal ions, pH, reaction time, temperatures, and types of reducing agents. For example, the plate-like CeO_2 could be fabricated by employing fresh egg white (Kargar et al. 2015; Maensiri et al. 2007), in which ovalbumin/lysozyme (egg proteins) were demonstrated to serve the function of bio-capping/stabilizing agent. Alternatively, several investigations on the plant-mediated synthesis of CeO_2 NPs using the extract of *Hibiscus sabdariffa* flower, *Petroselinum crispum* leaf and *Olea europaea* leaf as phyto-chelating/capping agents were also reported (Thovhogi et al. 2015; Korotkova et al. 2019; Maqbool 2017). Additionally, Thakur et al. (2019) were able to produce spherical CeO_2 (5–20 nm) by using the culture filtrate of *Curvularia lunata*. As depicted in Table 25.6, various exemplars on the bio-directed fabrication of CeO_2 NPs are also introduced.

Table 25.6 Different types of CeO_2 NPs obtained from the biological synthetic pattern

Capping agent	Cerium precursor	Particle size (nm)	Morphology of NPs	References
Egg white	Cerium(III) acetate	6–30	Plate-like	Maensiri et al. (2007)
Gloriosa superba	Cerium(III) chloride	5	Spherical	Arumugam et al. (2015)
Ricinus communis leaf extract	Cerium(III) chloride	34	Irregular	Suvetha Rani (2020)
Honey	Cerium(III) nitrate	23	Cubic	Darroudi et al. (2014)
Aspergillus niger culture filtrate	Cerium (III) chloride	5–20	Cubic-spherical	Gopinath et al. (2015)

25.2.2.1 Nanostructured CeO_2 from the Co-precipitation Method

In 2015, Safaei-Ghomi et al. (2015a) reported the application of CeO_2 derived from the co-precipitation of $Ce(NO_3)_3.6H_2O$ with NH_3 as an effective nanocatalyst for the assembly of 2-aminocyclohex-1-ene-1-carboxylic esters (Scheme 25.6).

Later, the co-precipitated CeO_2 NPs was also deployed to facilitate the room-temperature synthesis of polysubstituted dihydropyridines from the four-component coupling of aromatic aldehydes, ethyl cyanoacetate, arylamines and dimethyl acetylenedicarboxylate (Safaei-Ghomi et al. 2015b). In this study, the CeO_2 with particles size of 11 nm showed the superior activity over other nanosized catalysts such as CaO (35 nm), ZnO (24 nm), CuO (40 nm), MgO (18 nm) and SnO (28 nm), therefore enabling for high yields of polysubstituted dihydropyridines. As shown in the Scheme 25.7, the CeO_2-mediated coupling followed a set of sequential reactions of Knoevenagel condensation/Michael addition/annulation/tautomerization.

Subsequently, a high-yielding process of C-tethered bispyrazol-5-ols from the CeO_2-mediated multicomponent condensation of dimethyl acetylenedicarboxylate, phenylhydrazine and aromatic aldehydes in water was described by Safaei-Ghomi et al. (2015c). In this setting, the excellent activity of lab-prepared CeO_2 NPs was attributed to the high surface area (33.2 m^2/g) with respect to that of bulk CeO_2 (5.2 m^2/g), CaO (1.2 m^2/g) and ZrO_2 (4.9 m^2/g). Another reason came from the high distribution of oxygen vacancies as Lewis acidic sites on the surface of lab-designed CeO_2 NPs. On account of these factors, the CeO_2 NPs was able to produce derivatives of C-tethered bispyrazol-5-ol in high isolated yields (Scheme 25.8).

Likewise, Safaei-Ghomi et al. (2016) also introduced CeO_2 as a recyclable nanocatalyst for the *mechanochemical* synthesis of 2-amino-4,6-diarylbenzene-1,3-dicarbonitriles. As depicted in Scheme 25.9, the CeO_2-mediated reaction is suggested to undergo a mechanistic sequence of Knoevenagel condensation/Michael addition/annulation/aromatization at room temperature.

Later, D'Alessandro et al. (2015) described the usefulness of CeO_2 in triggering the solvent-free multicomponent Hantzsch reaction. Remarkably, it is revealed that a switchable construction of 1,4-dihydropyridine and 2-phenylpyridine could be

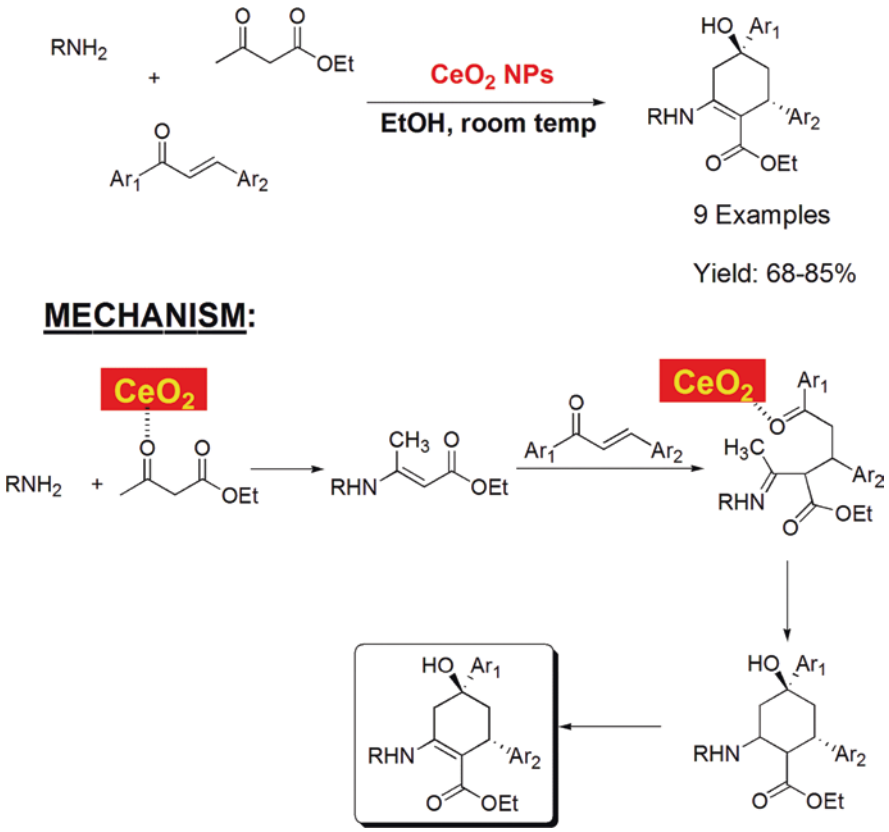

Scheme 25.6 Room-temperature synthesis of 2-aminocyclohex-1-ene-1-carboxylic esters over CeO_2 NPs

accomplished from the coupling of benzaldehyde, methyl acetoacetate and ammonium acetate under different temperatures. Remarkably, it is found that 97% yield of phenylpyridine was generated at 25 °C, while elevating the reaction temperature to 80 °C offered 75% yield of 1,4-dihydropyridine. In both cases, the recovered CeO_2 NPs could maintain the original activity after four consecutive trials. Similarly, Suresh et al. (2016) disclosed that a novel scaffold of fused triazolo/tetrazolo[1,5-*a*]pyrimidine could be assembled under the catalysis of CeO_2 NPs. In this manner, the CeO_2-mediated condensation of substituted aromatic aldehydes, benzoylacetonitrile with 5-aminotriazole/5-aminotetrazole, took place smoothly in water to generate two types of fused pyrimidine products. The catalytic role of CeO_2 NPs in this tandem Knoevenagel/Michael addition/intermolecular cyclization/intermolecular dehydrogenation reaction is clearly clarified in Scheme 25.10.

In another example, Gharib et al. (2013) fabricated the nanostructured CeO_2 by precipitating the aqueous solution of $(NH_4)_2Ce(NO_3)_6$ with NH_3. Thanks to the high surface area, the lab-designed CeO_2 was capable of promoting the *aqueous-phase*

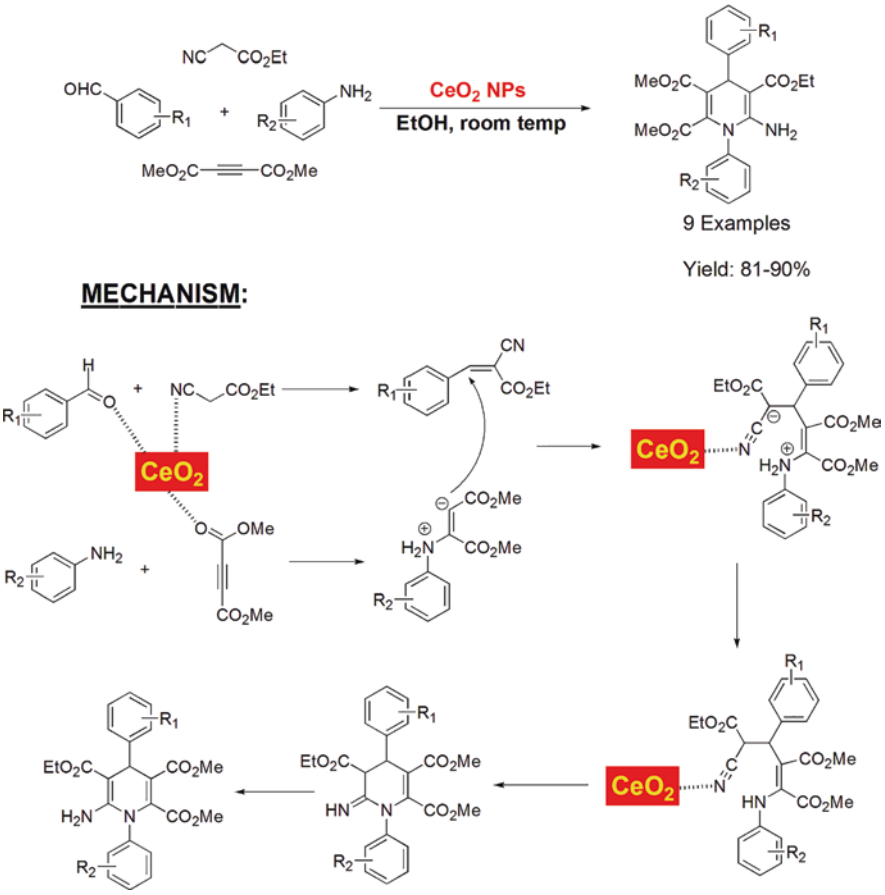

Scheme 25.7 Construction of polysubstituted dihydropyridines over CeO_2 NPs

coupling of Lawsone reagent with 3-methyl-1-phenyl-1*H*-pyrazol-5-amine and substituted benzaldehydes under reflux condition. Accordingly, seven derivatives of 3-methyl-1-phenyl-1*H*-benzo[*g*]pyrazolo[3,4-*b*]quinoline-5,10-diones could be furnished in good to excellent yields (66–94.5%).

To construct the multiple heterocyclic scaffold of imino-pyrrolidine-thione, Wang et al. (2016) applied the porous CeO_2 nanorods obtained from the hydrothermal treatment of $Ce(NO_3)_3.6H_2O$ with $(NH_4)_2CO_3$ to mediate the coupling of 2-mercaptobenzoxazole/2-mercaptobenzothiazole with a mixture of substituted benzaldehydes, malononitrile and isocyanide. As illustrated in Scheme 25.11, the Ugi four-component condensation could run smoothly in a binary mixture of CH_3CN-H_2O (3:1, *v/v*) with 5 mol% of nanoporous CeO_2 to deliver a broad library of imino-pyrrolidine-thiones. Under identical condition, commercial and other synthetic CeO_2 NPs with different morphologies (i.e. linear, granular and fusiform) were found to give lower yield of coupling product with respect to the titled

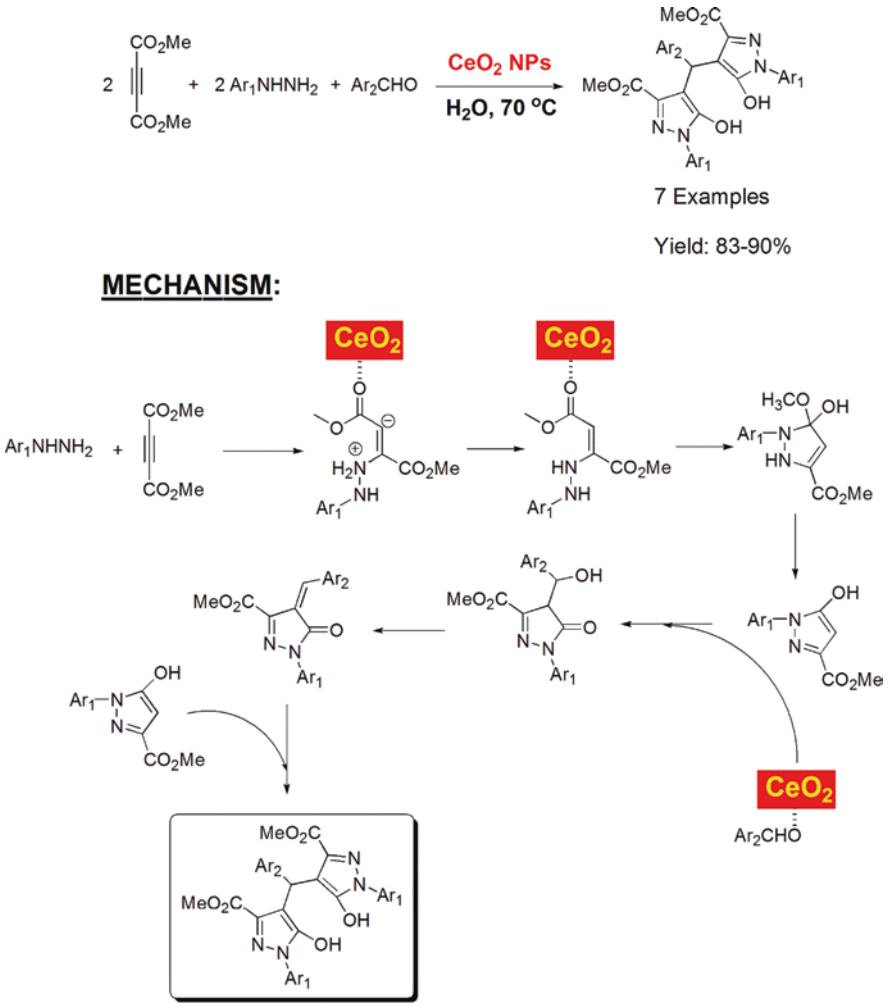

Scheme 25.8 Construction of C-tethered bispyrazol-5-ols over CeO_2 NPs

nanoporous CeO_2. Unfortunately, the loss of oxygen storage in the spent CeO_2 was assumed to take place, thereby leading to a significant drop in the catalytic performance after the third recycle.

To address intrinsic drawbacks in the current manufacture of azole compounds (benzimidazoles, benzothiazoles and benzoxazoles), Shelkar et al. (2013) established a facile and eco-friendly strategy to construct these privileged skeletons upon employing CeO_2 nanocatalyst prepared from the surfactant-assisted co-precipitation under ultrasonic irradiation (Terribile et al. 1998). In comparison with other tested metal oxides (i.e. ZnO, TiO_2, MnO_2, SiO_2, Al_2O_3, La_2O_3 and Cu_2O NPs), the robust CeO_2 NPs displayed the preeminence in fostering high yields of benzimidazoles,

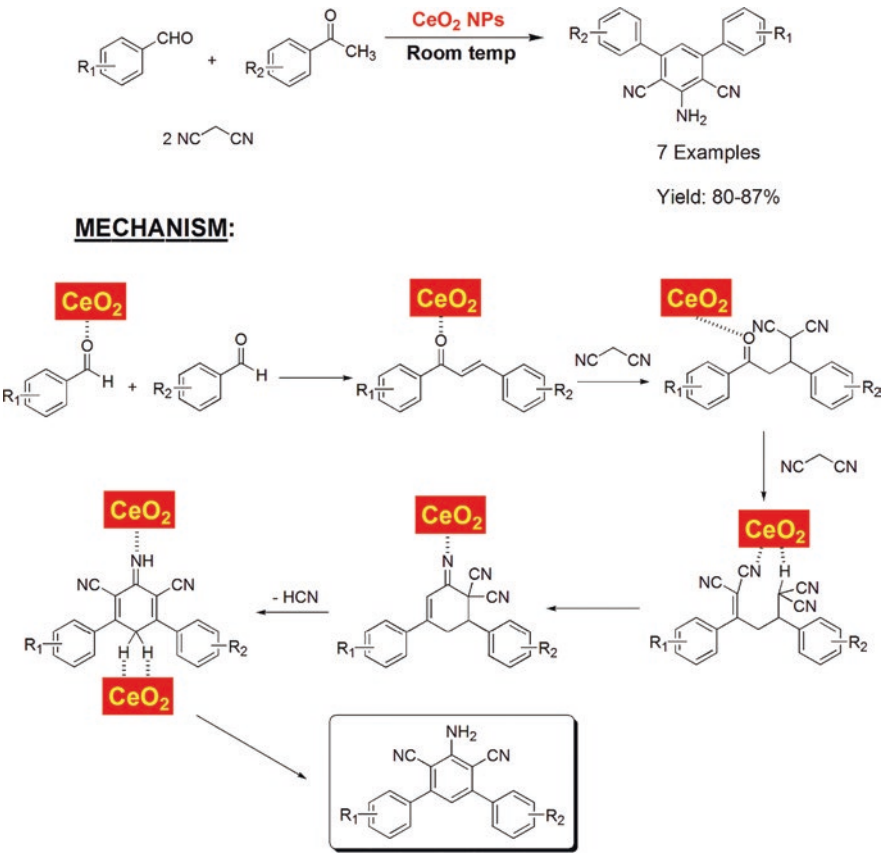

Scheme 25.9 Solvent-free access of 2-amino-4,6-diarylbenzene-1,3-dicarbonitriles over CeO_2 NPs

benzothiazoles and benzoxazoles from the aqueous-phase coupling of 1,2-phenylenediamine/2-aminothiophenol/2-aminophenol with aldehydes, respectively (Scheme 25.12).

25.2.2.2 Nanostructured CeO_2 from the Polymer-Directed Method

In 2011, Girija et al. (2011) fabricated the polymer-directed CeO_2 nanoparticles by treating the mixture of $(NH_4)_2Ce(NO_3)_6$, hexylamine and polyethylene glycol 6000 (PEG-6000) under microwave irradiation, which was then examined for the catalytic assembly of polyhydroquinolines. In this context, the solvent-free multicomponent condensation of aldehydes, ethyl acetoacetate, dimedone and ammonium acetate was carried out under the assistance of both microwave radiation and CeO_2 NPs, finally providing 88–97% yields of target polyhydroquinolines. However, a

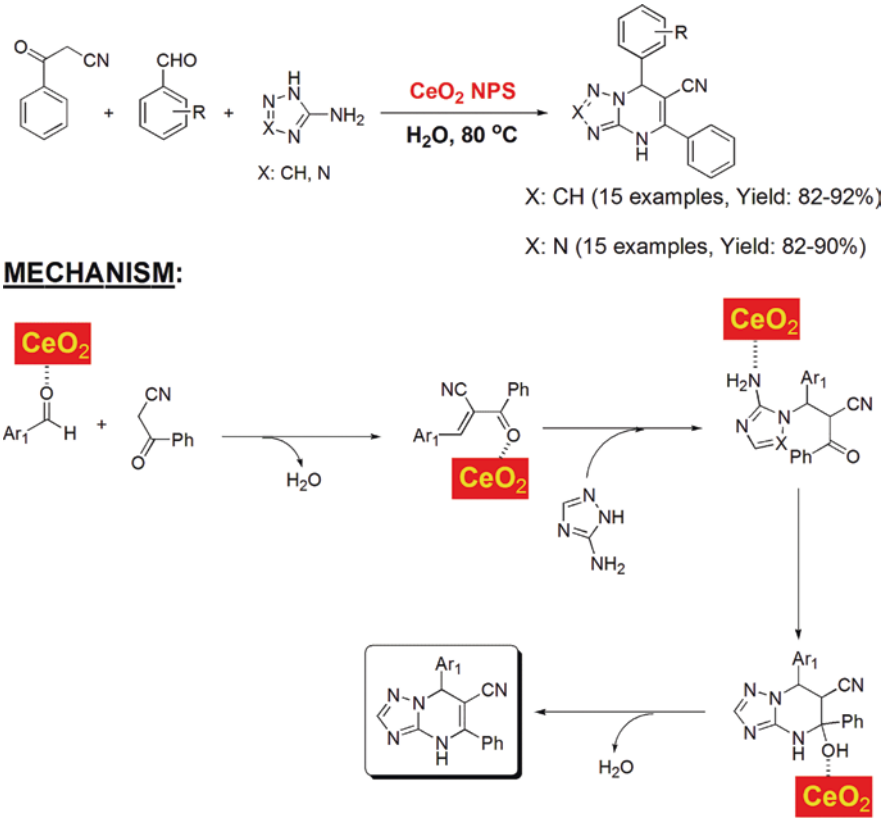

Scheme 25.10 Construction of fused triazolo/tetrazolo[1,5-*a*]pyrimidines over CeO_2 nanocatalyst

gradual loss in the catalytic activity of recovered CeO_2 was observed due to the slow oxidation of Ce NPs during the recycling trials.

By combining the reverse microemulsion system of bis(2-ethylhexyl) sulfosuccinate-lecithin-isooctane-water with different polymers of polyvinylpyrrolidone (PVP), block copolymer P123 or reverse block copolymer 17R4 as structural controller during the preparative procedure, Samai et al. (2016) were able to prepare a set of CeO_2 (i.e. CeO_2-PVP; CeO_2-P123; and CeO_2-17R4) with controlled nanoparticle sizes. Noticeably, it is uncovered that the relationship between the morphology and the catalytic performance of these titled nano-CeO_2 was intimately correlated with the directing polymeric agents. In this aspect, CeO_2-PVP with the largest surface area (58.0 m^2/g) displayed superior results in comparison with CeO_2-P123 (45 m^2/g) and CeO_2-17R4 (40.96 m^2/g) upon coupling nitrostyrene, 1,3-dicarbonyl compounds and aromatic primary amines. Accordingly, a collection of *N*-aryl pyrroles in the range yields of 59–77% was successfully produced over recyclable CeO_2-PVP nanocatalyst.

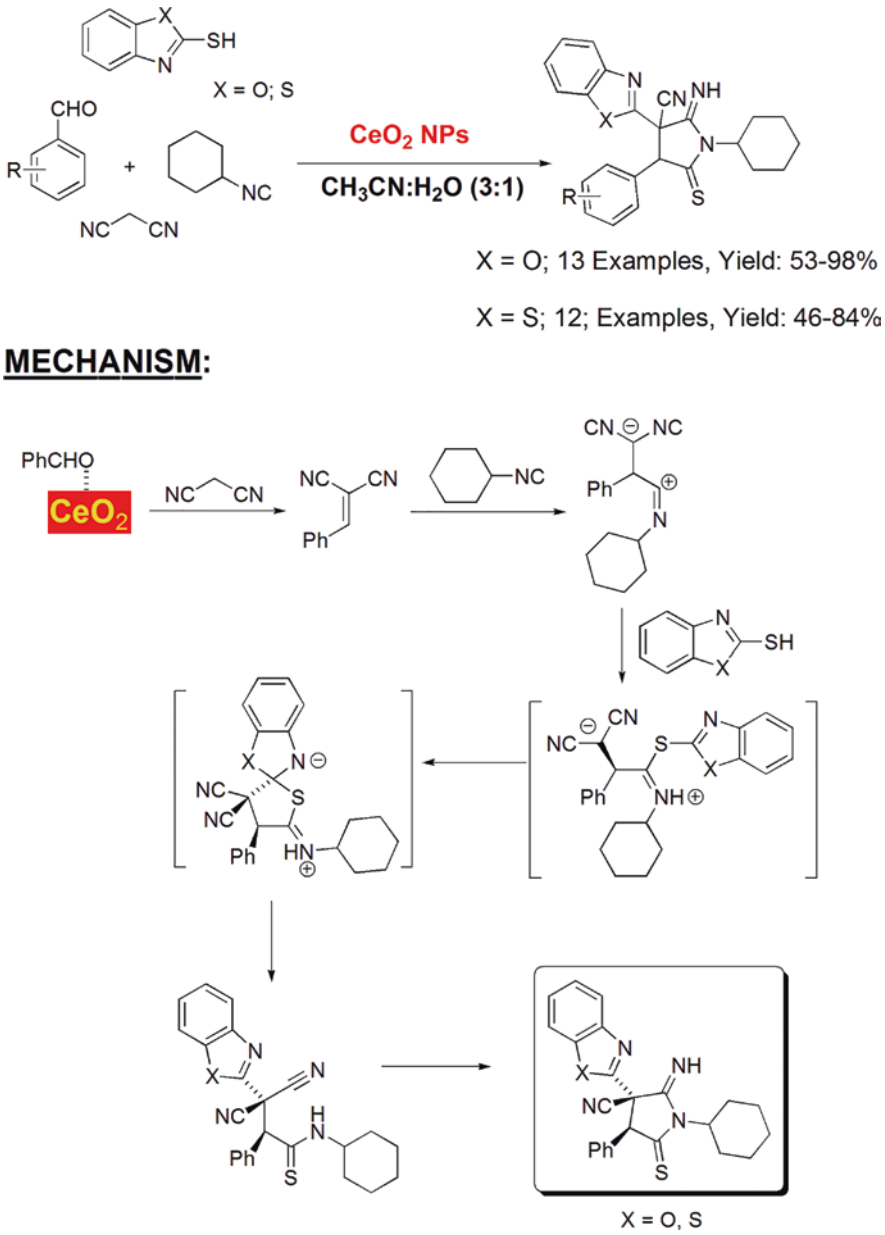

Scheme 25.11 Multicomponent synthesis of imino-pyrrolidine-thiones over CeO_2 nanoparticles

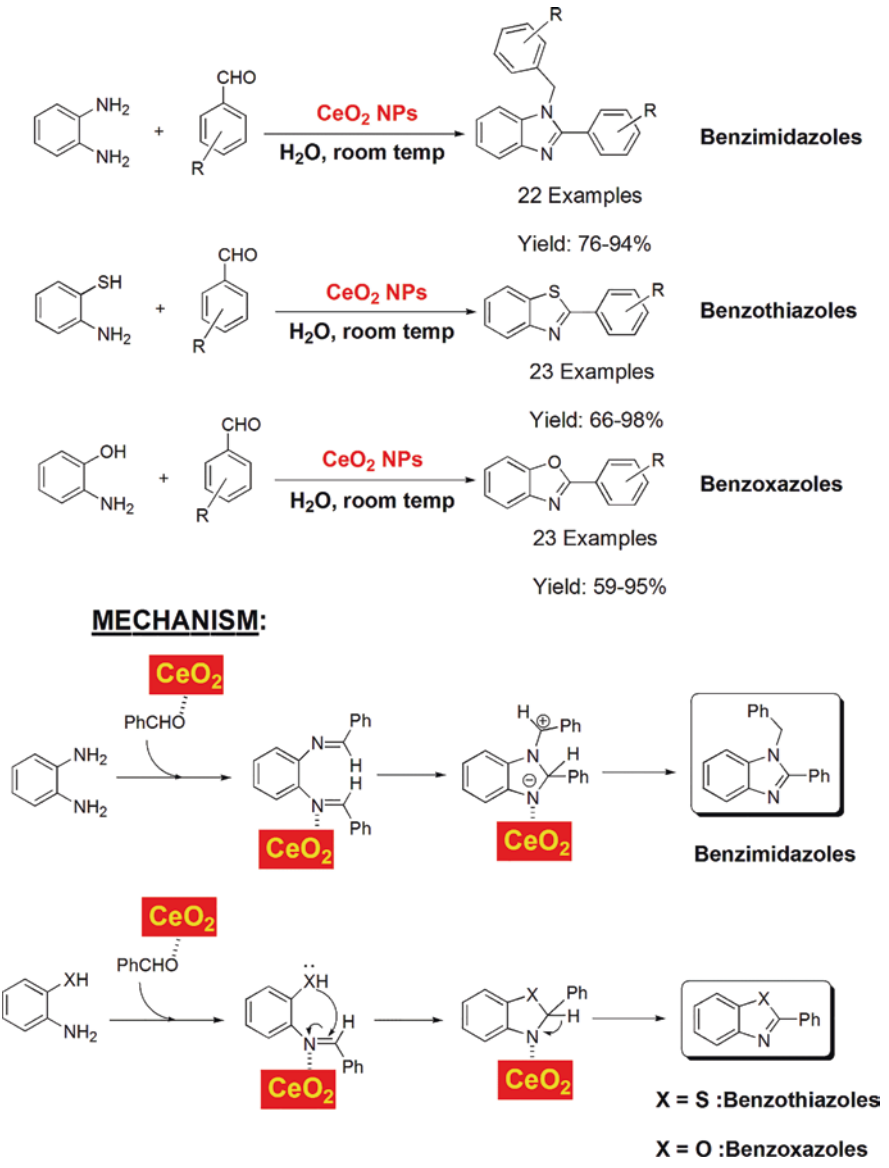

Scheme 25.12 Nano-CeO_2-mediated synthesis of benzimidazoles, benzothiazoles and benzoxazoles

25.2.2.3 Nanostructured CeO_2 from the Biology-Directed Method

Recently, plant extracts or bio-based materials have been deployed as greener alternatives to chemical reductants/oxidants/precipitating agents (e.g. cetyltrimethylammonium bromide, polyethylene glycols, monoethanolamine, ammonium hydroxide

and polyvinylpyrrolidone) in the fabrication of ceria nanoparticles (Arumugam et al. 2015; Ferreira et al. 2016). With these nature-derived compounds, the preparative procedure can circumvent a complicated and tedious purification process (washing, calcination, Soxhlet extraction, etc.) to deliver organic-free CeO_2 NPs. Prompted by these examples, Zamani et al. (2018) explored the walnut shell powder to assist the fabrication of nano-CeO_2 in the absence of any surfactants or precipitating agents, in which the particle size could be tuned by controlling the ratio of Ce source/biomass. In this case, it is found that the presence of walnut shell as a cheap and green template is necessary to trigger smaller size of ceria, where the optimal ratio of Ce source/biomass was established at the ratio of 6.9:10. Hence, the resulting CeO_2 with a particle size of 9 nm was able to stimulate the aqueous-phase coupling of *o*-phenylenediamine and acetone with *tert*-butyl isocyanide at 80 °C to give 93% yield of 3,4-dihydroquinoxalin-2-amine.

25.2.3 Cerium Mixed Oxides

There are several documented methods for fabricating mixed metal oxides such as co-precipitation, wet impregnation, sol-gel, hydrothermal treatment, etc. (Courty and Marcilly 1976; Cousin and Ross 1990). In such cases, various true mixed oxides or solid solutions with the deposition of different metals can be readily composed to render a set of binary, ternary, quaternary or multiple-component mixed metal oxides, respectively. Undoubtedly, the mixed metal oxides display distinctive properties of acidity-basicity, oxidation-reduction, morphology (e.g. particle size, pore volume, surface area and defect) and thermal/chemical stability in comparison to pure metal oxides (Grzybowska-Swierkosz 1987; Wang et al. 2017). In addition, the bonding network between metals in mixed oxides allows the reagents to approach the active sites in an effective and selective manner, therefore increasing the yield and selectivity of the target products (Gawande et al. 2012; Burange and Gawande 2016). Thanks to these prominent features, the cerium-based mixed oxides have been widely deployed in the production of chemicals, organic synthesis, combustion of pollutants and energy applications (Orge et al. 2012; Shen et al. 2009; Zhang et al. 2018; Liu et al. 2019; Melchionna and Fornasiero 2014). For example, the nanocomposite of CeO_2-ZrO_2 obtained by the co-precipitation gave 90% yield of acetophenone from the deprotection of acetophenone oxime, whilst the pure CeO_2 only delivered 60% yield under identical condition (Deshpande et al. 2008). In another case, the catalytic activity of $Mn_3Gd_{7-x}Ce_x(SiO_4)_6O_{1.5}$ in the degradation of tetracycline was improved by the introduction of cerium in the structure, ascribable to the generation of active sites, the redox potential and an increase in the oxygen storage capacity (Fu et al. 2019). Likewise, Albadi et al. reported the practicality of CuO@CeO_2 nanocomposite for the construction of various heterocyclic structures through the multicomponent patterns (Scheme 25.13). Towards this end, the CuO@CeO_2 catalyst was composed from the co-precipitation of KOH with an aqueous mixture of $Ce(NO_3)_3$ and $Cu(NO_3)_2$. In the presence of CuO@CeO_2 nanocatalyst,

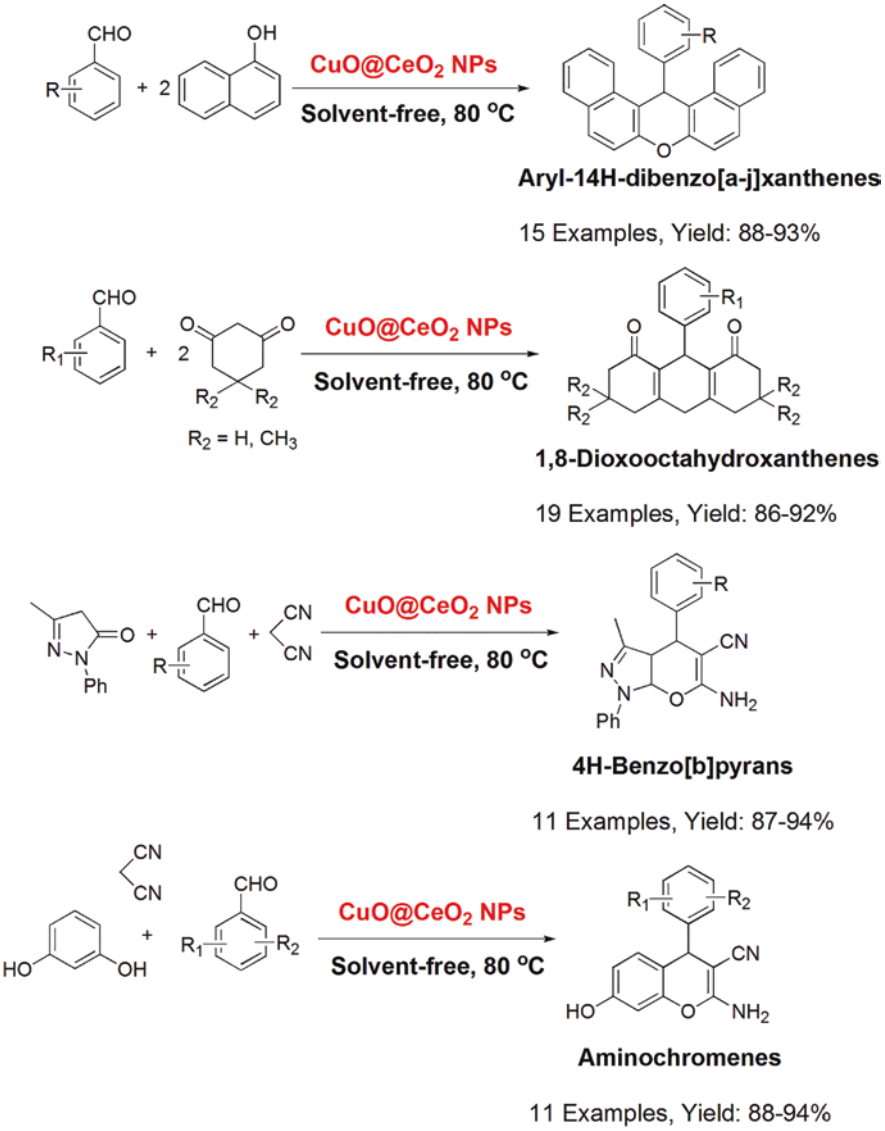

Scheme 25.13 Solvent-free synthesis of various heterocycles over $CuO@CeO_2$ nanocomposite

the solvent-free assembly of aryl-14*H*-dibenzo[a-j]xanthenes (Albadi et al. 2013a), 1,8-dioxooctahydroxanthenes (Albadi et al. 2013b), 4*H*-benzo[b]pyrans (Albadi et al. 2013c) and aminochromenes (Albadi et al. 2013d) was achievable with no difficulty.

Besides, Albadi et al. (2014a) also applied the nanostructured CuO@CeO_2 as a heterogeneous Lewis acid to induce the assembly of biscoumarins from benzaldehydes and 4-hydroxycoumarin in water (Scheme 25.14).

To develop a benign protocol for 1,4-disubstituted-1,2,3-triazoles, Albadi et al. (2014b) deployed the amberlite-supported azide as an alternative source of azide ion and CuO@CeO_2 as a heterogeneous copper catalyst. In this regard, the CuO@CeO_2-mediated click synthesis of functionalized triazoles by refluxing a mixture of aryl terminal alkynes and α-bromo ketones/ benzyl bromides with amberlite-supported azide in ethanol could provide excellent isolated yields of various triazoles in an eco-friendly manner (13 examples, 88–92%). In such examples, it is verified that the robust CuO@CeO_2 with no leeching of Cu could retain the outstanding catalytic activity after several recycling trials.

Furthermore, the practicality of nanostructured MgO@CeO_2 as an active solid catalyst in the construction of heterocyclic skeletons was also recognized (Scheme 25.15). In this setting, a collection of imidazo[4,5-c]pyrazoles (Moydeen et al. 2017), 2-amino-4-arylthiophene-3-carboxamides and thieno[2,3-*d*]pyrimidin-4(3*H*)-one-s (Shafighi et al. 2018) could be furnished in a high efficacy. After several recycles, no significant loss in the performance of recovered MgO@CeO_2 was observed, indicating the robustness of this titled nanocatalyst during the transformation.

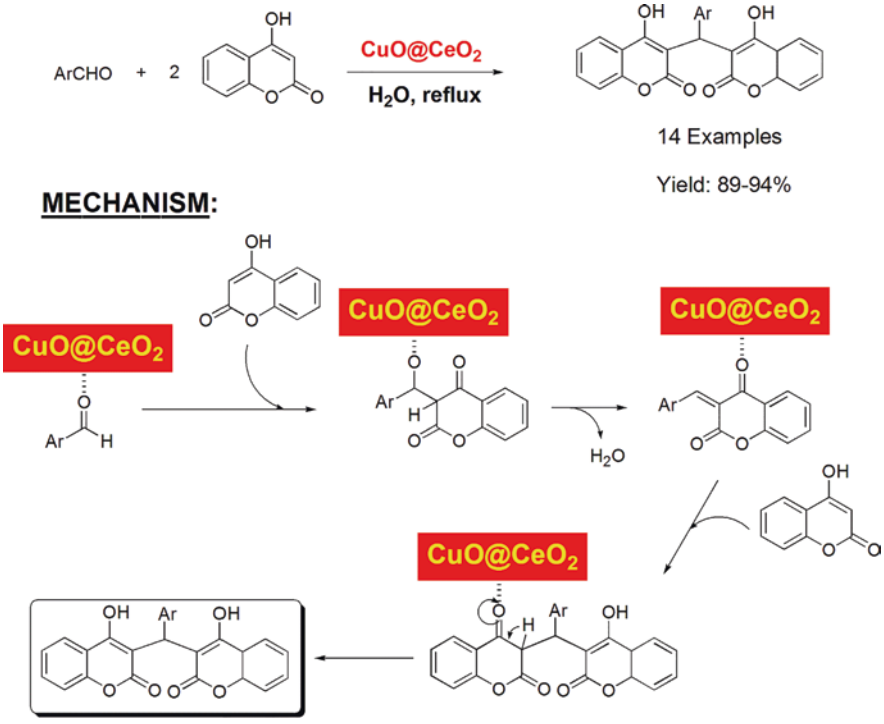

Scheme 25.14 Synthesis of biscoumarin derivatives over CuO@CeO_2 nanocatalyst

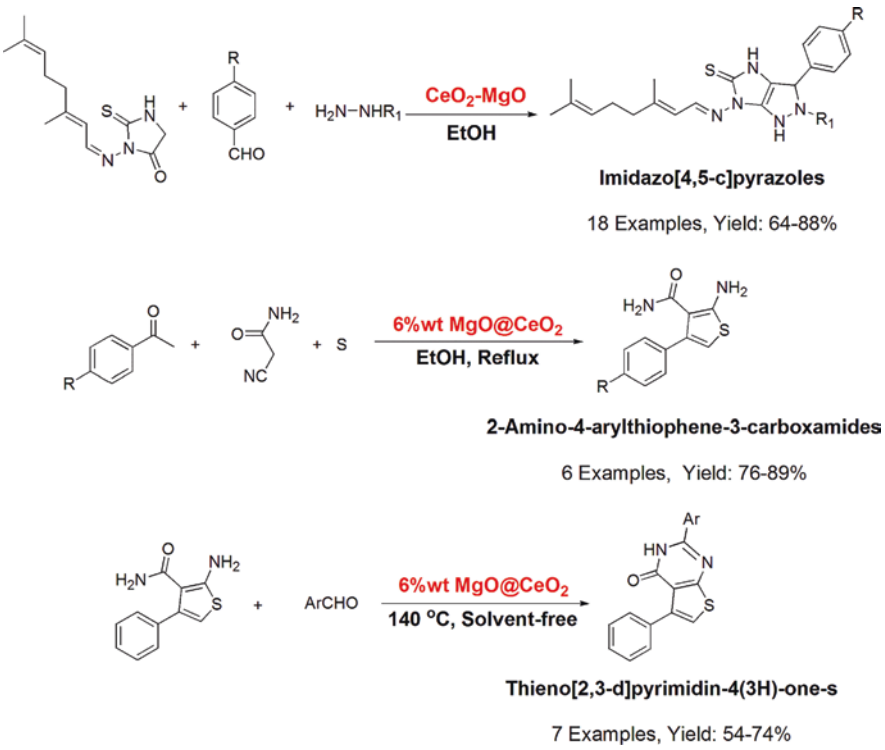

Scheme 25.15 Preparation of diversified heterocycles *over* $MgO@CeO_2$ nanocatalyst

In 2016, Vijay Kumar et al. (2016) designed the $Eu_2O_3@CeO_2$ nanocomposite for the multicomponent synthesis of phenyldiazenylacridinedione-carboxylic acids. For that objective, the binary oxide was prepared from the co-precipitation of $Ce(NO_3)_3$ and $Eu(NO_3)_3$ with NH_3 solution upon setting the optimal molar of Ce/Eu at a value of 8:2. The structural analysis indicated that the introduction of Eu on CeO_2 helped to induce the oxygen defects and to increase the surface area, leading to the superior catalytic activity of $Eu_2O_3@CeO_2$ over pure CeO_2. Hence, the catalysis of $Eu_2O_3@CeO_2$ in the aqueous-phase coupling of 1,3-dicarbonyl compounds, 4-hydroxy-3-methoxy-5-(substituted-phenyl-diazenyl)-benzaldehydes with glycine, enabled high yielding of (4-hydroxy-3-methoxy-5-(substituted-phenyldiazenyl)-dihydropyridineacetic acids. As described in the Scheme 25.16, $Eu_2O_3@CeO_2$ served as a heterogeneous Lewis acid in activating the C=O bonds during the multicomponent synthesis.

In another study, Ghayour et al. (2018) introduced $ZnO@CeO_2$ with 30.1 wt% of ZnO for the solvent-free coupling of aldehydes with 2-amino-4,5,6,7-tetrahydrobenzo[*b*]thiophene-3-carboxamide, where 62–92% yields of the thieno[2,3-*d*]pyrimidin-4(3*H*)-ones were achievable. To stimulate the construction of novel chromene derivatives bearing azo segment, Sagar Vijay Kumar et al. (2016)

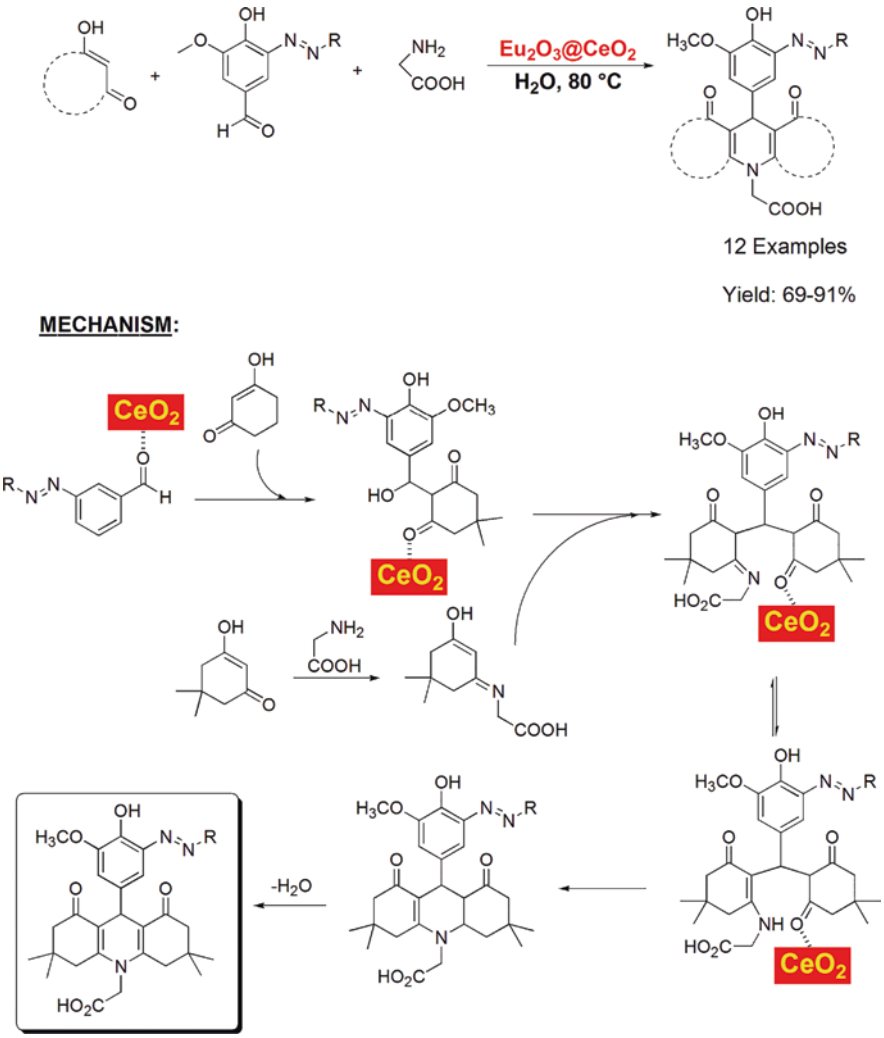

Scheme 25.16 Preparation of phenyldiazenyl-acridinedione-carboxylic acid derivatives from the Eu_2O_3@CeO_2-mediated multicomponent reaction

devised the co-precipitated nanocomposite of ZrO_2@CeO_2 (ratio Zr/Ce = 1:1) as a potential candidate for the room-temperature condensation of malononitrile, 4-hydroxy-3-methoxy-5-(substituted-phenyl-diazenyl) benzaldehydes with different compounds of 1,3-dicarbonyls. The mechanistic pathway leading to the formation of 2-amino-4-(4-hydroxy-3-methoxy-5-(substituted-phenyl-diazenyl)-chromene-3-carbonitriles is assumed to follow a set of Knoevenagel condensation/Michael addition/tautomerization/annulation reaction, in which ZrO_2@CeO_2 helped to activate the C=O and C ≡ N bond (Scheme 25.17).

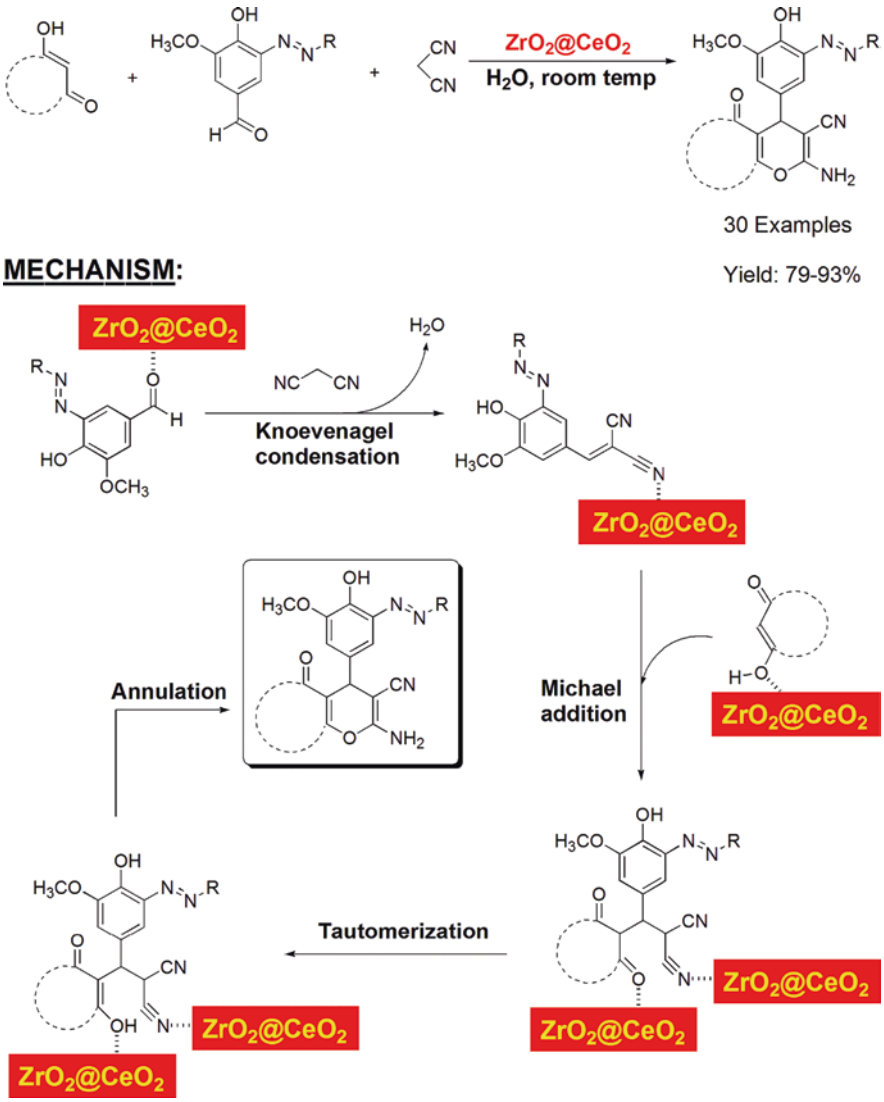

Scheme 25.17 Synthesis of novel azo chromenes over ZrO_2@CeO_2

Another exemplar of cerium-based mixed metal oxides comes from the preparation of $Ce_1Mg_{0.6}Zr_{0.4}O_2$ composite as reported by Rathod et al. (2010). In this scenario, the aqueous mixture of $(NH_4)_2Ce(NO_3)_6$, Mg $(NO_3)_2$ and $Zr(NO_3)_2$ was co-precipitated with NH_3 and PEG-400, followed by calcination at 500 °C to render the titled nanocomposite. Through the structural characterization, the authors claimed that all three metals (Ce, Mg and Zr) in $Ce_1Mg_{0.6}Zr_{0.4}O_2$ had a strong mutual interaction and were highly dispersed on the surface. Besides, the insertion of

magnesium into the lattice of cerium-zirconium led to a decrease in the size of particles along with an enhancement in the acidic-basic active sites, thereby enhancing the efficiency of $Ce_1Mg_{0.6}Zr_{0.4}O_2$ NPs in promoting the construction of tetrahydrobenzo[*b*]pyrans. By refluxing the mixture of substituted benzaldehydes, malononitrile and dimedone with $Ce_1Mg_{0.6}Zr_{0.4}O_2$ in ethanol, the authors were able to obtain excellent yields of corresponding pyran derivatives (10 examples, yield: 90–94%).

Besides, cerium is also treated as a metal dopant in some metal oxides to improve the catalytic performance of these materials in various transformations (Fu et al. 2019; Fayaz et al. 2016; Do et al. 2018). For instance, 5 wt% CeO_2 doped on NiMnO (calcined at 400 °C) could induce 100% conversion of benzyl alcohol to benzaldehyde (Sultana et al. 2015). Doping 2.5 wt% of ceria on $CuMnO_x$ helped to improve the efficacy of the catalyst in the low temperature oxidation of CO (Dey and Dhal 2020). Likewise, Samantaray et al. (2012) prepared a set of CeO_2@CaO nanocomposites by the citrate method and introduced them as main catalysts for the access of aminochromenes. It is revealed that the amorphous citrate template enabled the generation of macropores on the surface of resulting porous materials, in which the phase of binary oxide with the particle size of 5–25 nm was well dispersed in the phase of calcia. Furthermore, the incorporation of Ce^{4+} into the lattice of CaO might also increase the active basic sites on the surface of CeO_2@CaO composites, thereby improving their catalytic capability with respect to that of pure CaO. In this study, the authors stated that the CeO_2@CaO with 20 mol% of CeO_2 displayed the supreme performance in providing a structural diversity of 2-amino-2-chromenes (10 examples, yield: 76–85%) upon treating a mixture of substituted benzaldehydes and malononitrile with α-napthol in water at 80 °C. Meanwhile, Maddila et al. (2016) explored the recyclable cerium-vanadium-loaded alumina catalyst (Ce-V@Al_2O_3) for the solvent-free synthesis of multisubstituted pyridines. Herein, setting the total loading of Ce-V on the Al_2O_3 support at 2.5 wt% was verified to offer the best result thanks to the optimal distribution of acidic-basic sites on the surface of hybrid catalyst. Accordingly, the room-temperature manufacture of functional pyridines from aromatic aldehydes, malononitrile and ethanol was accomplished in a facile and selective manner (11 examples, yield: 86–94%). Subsequently, CeO_2@ZrO_2 was developed as an effective catalyst to induce the four-component annulation of substituted benzaldehydes, malononitrile and hydrazine hydrate with ethyl acetoacetate at room temperature, where a broad library of pyrano[2,3-c]pyrazole was rendered in the range yields of 89–98% (Maddila et al. 2017a). Alternatively, Khan et al. (2019) reported the high-yielding formation of quinolines from the CeO_2@TiO_2-mediated coupling of anilines, aldehydes with acetophenone in solvent-free condition.

In most cases, a proper choice of solvent to dissolve the product, suction filtration or centrifugation must be employed to separate the heterogeneous catalyst from the reaction mixture, causing great annoyances during the catalyst recovery. To overcome these barriers, magnetically recoverable nanocatalysts would become more ideal in terms of “green chemistry” viewpoint (Polshettiwar et al. 2011). In this aspect, superparamagnetic Fe_3O_4 (magnetite) which is considered as a cheap,

stable and easy-to-prepare support has been widely implemented to immobilize active catalysts in many reactions (Gawande et al. 2013a; Sharma et al. 2016b), since the active catalyst@Fe_3O_4 composite would be easy to recover from the reaction medium by an external magnet. Motivated by these works, Gawande et al. (2013b) designed a magnetic nanocatalyst of magnetite-ceria (CeO_2@Fe_3O_4) for the room-temperature construction of dihydropyridines and tetrahydropyridine (Scheme 25.18). Similarly, Shelkar et al. (2015) designed CeO_2@Fe_3O_4 with 7.44 wt% of Ce as a cheap and active nanocatalyst for the C-H functionalization of heteroarenes (Scheme 25.19). In this approach, the arylation was implemented by heating the mixture of benzoxazole/benzothiazole (1 equiv.) and aryl halides (1 equiv.) with K_2CO_3 (2 equiv.) in DMSO under the assistance of 5 mol% of CeO_2@Fe_3O_4, which led to a myriad of 2-aryl-substituted derivatives of benzoxazole and benzothiazole.

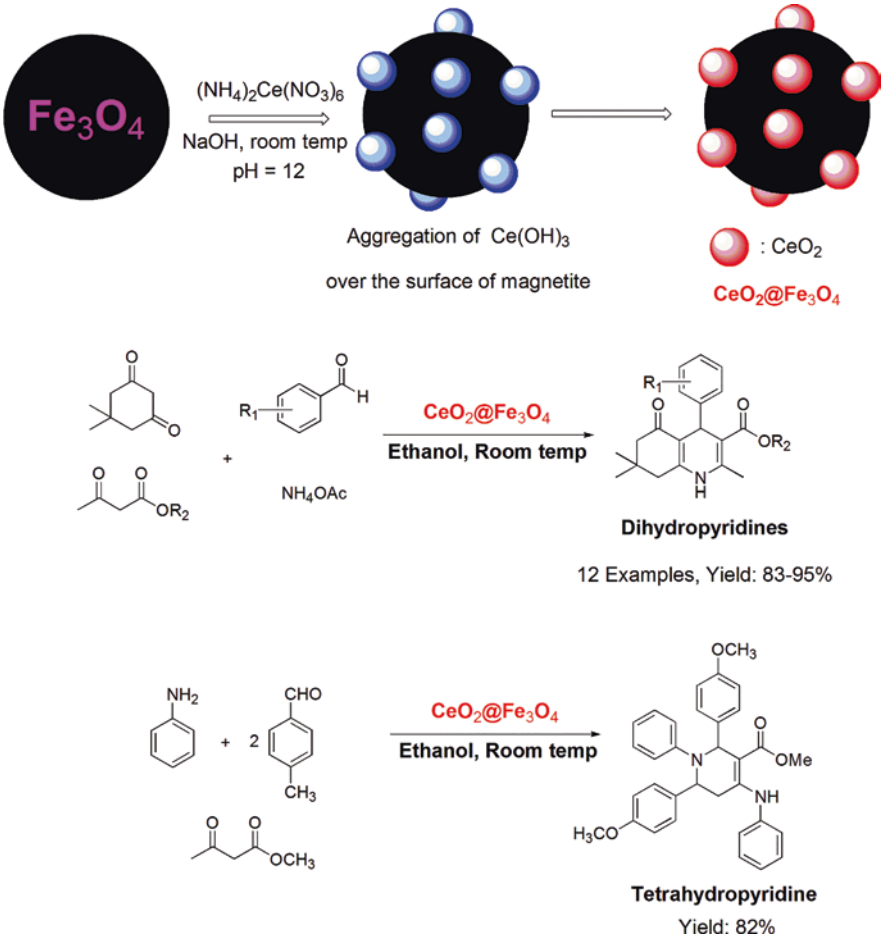

Scheme 25.18 Fabrication and utility of CeO_2@Fe_3O_4 in the manufacture of dihydropyridines and tetrahydropyridine

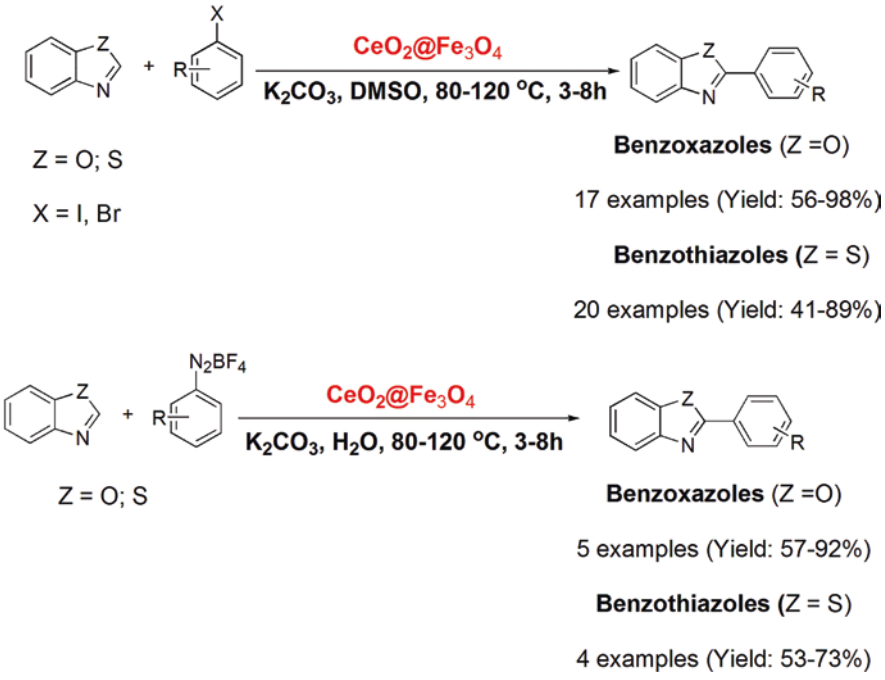

Scheme 25.19 C-H functionalization of benzoxazoles and benzothiazoles over magnetic CeO_2@Fe_3O_4 nanocatalyst

Strikingly, the CeO_2@Fe_3O_4-mediated *N*-arylation could be accomplished in greener condition by replacing the mixture of aryl halides-DMSO with a cheap combination of arenediazonium salts and water. In those examples, the magnetic CeO_2@Fe_3O_4 nanocatalyst could be readily recovered and recyclable for several batches with a negligible deactivation.

25.2.4 Cerium-Solid Material Composite

25.2.4.1 CeO_2-Polymer

In 2005, Sabitha and Shailaja (2005, 2008) designed a hybrid catalyst composed of CeO_2 NPs and polymer to promote the assembly of heterocycles. For this target, the titled composite, CeO_2@(VP-co-DVB), was readily prepared from the suspension copolymerization of 4-vinylpyridine (VP), 1,4-divinylbenzene (DVB) and $CeCl_3$ in basic condition upon using polyvinylpyrrolidone K30 as a removable template and an initiator mixture of Lupersol TAEC/Luperox 101 (Scheme 25.20). Strikingly, it is indicated that the robust CeO_2@(VP-co-DVB) catalyst could induce the synthesis

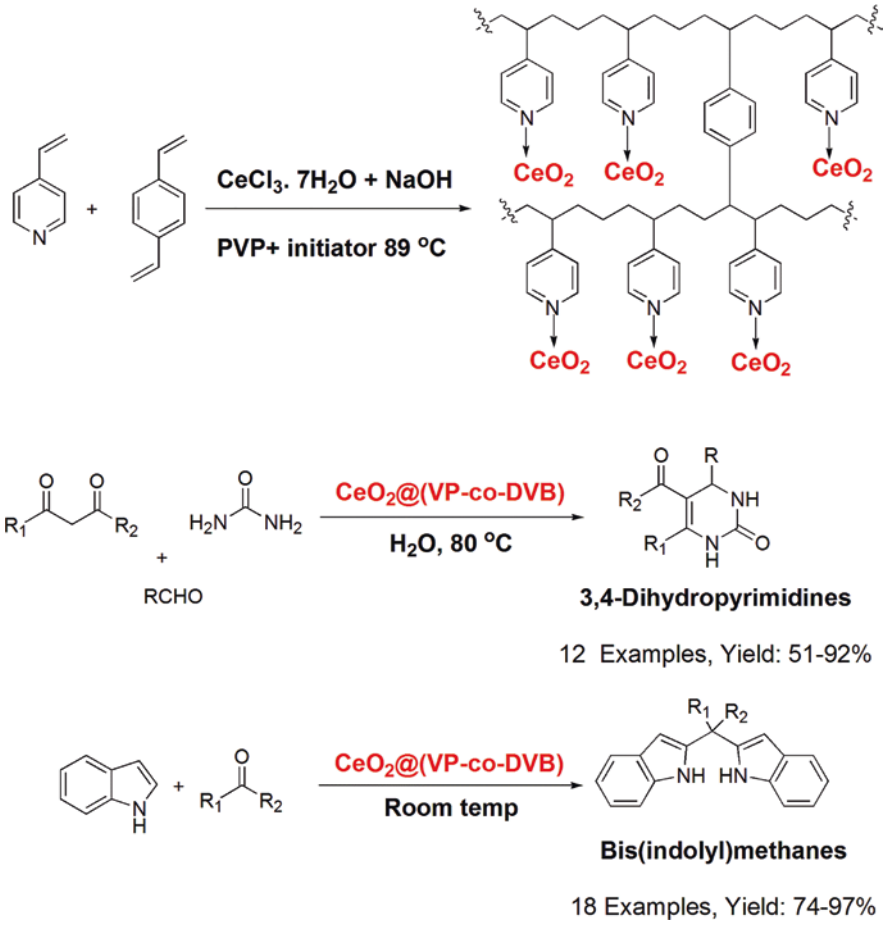

Scheme 25.20 Preparation and practicality of CeO_2@(VP-co-DVB) nanocatalyst in the synthesis of 3,4-dihydropyrimidines and bis(indolyl)methanes

of both 3,4-dihydropyrimidines (12 examples, yield: 51–92%) and bis(indolyl) methanes (18 examples, yield: 74–97%) in high efficacy after multiple recycles.

25.2.4.2 CeO_2-Silica

Generally, silica is acknowledged as a versatile solid material owing to its own specific properties of high surface area, high thermal stability and a great flexibility in pore sizes and acidic-basic sites (Agotegaray and Lassalle 2017). Accordingly, silica has been widely employed as an exceptional template to immobilize active species in a well-dispersed manner, therefore providing a great volume of powerful silica-supported catalysts in the domain of heterogeneous catalysis (Akelah 1981).

In this context, MCM41 and SBA15 are two exemplary mesoporous silica which have widespread applications as either heterogeneous catalysts or solid supports in various transformations (Bhattacharyya et al. 2006; Rahmat 2010). Owing to a large specific surface area along with a well-defined pore structure of the mesoporous template, active species (metals or metal complexes) can be incorporated and uniformly dispersed on the wall of mesopores of MCM41/SBA15 to deliver a plenty of active heterogeneous catalysts (Liang et al. 2017). For example, Akondi et al. (2012) successfully fabricated CeO_2@MCM-41 with 15 wt% of Ce (CeO_2@MCM-41) by the wet impregnation to facilitate the oxidative coupling of 2-naphthol with substituted anilines. Similarly, the excellent catalytic activity of CeO_2@MCM-41 in the manufacture of mono- and bis-dihydropyrimidin-2(1*H*)-ones (Vadivel et al. 2013), benzoxanthenones/benzochromenones (Akondi et al. 2014) and caprolactam (Babu et al. 2016) was also recorded (Scheme 25.21). In these cases, the immobilization of cerium on the inner surface of mesopores of parent MCM41 is accountable for the improvement in the stability and catalytic performance with respect to CeO_2. Besides, Saadati-Moshtaghin and Zonoz (2019) developed a novel three-component composite of Fe_3O_4-MCM41-CeO_2 as a new hybrid solid catalyst for the solvent-free manufacture of tetrahydobenzo[b]pyrans from the condensation of aromatic aldehydes, malononitrile and dimedone (15 examples, yield: 69–96%).

Apart from MCM41, silica (SiO_2) is also regarded as a versatile solid support in heterogeneous catalysis (Ramazani et al. 2017). From the perspective of economical metrics, no template-directed SiO_2 is considered cheaper and more

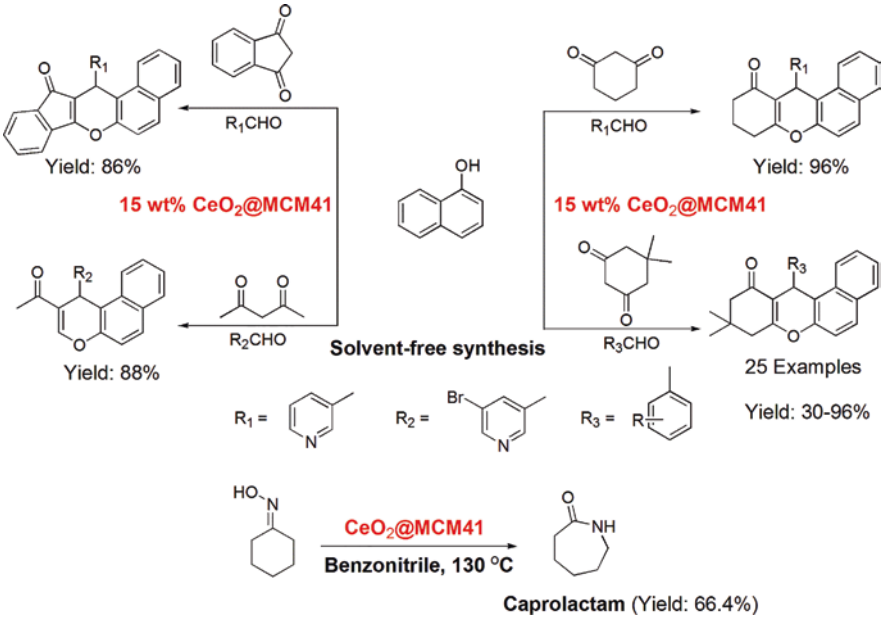

Scheme 25.21 Utility of CeO_2@MCM41 in the assembly of benzoxanthenones, benzochromenones and caprolactam

easy-to-prepare than MCM41. Moreover, the "sol-gel chemistry" is also acknowledged as a powerful tool in preparing metal oxides and oxide-supported metal catalysts (Esposito 2019). Prompted by these reasons, Akondi et al. (2016) later deployed sol-gel-derived SiO_2 in place of MCM41 to immobilize CeO_2 for the fabrication of nanostructured CeO_2@SiO_2. The textural analysis indicated that Ce^{4+} species from the oxidation of Ce^{3+} were successfully incorporated and tightly bound inside the mesoporous silica framework during the preparative procedure, thereby hampering the possible leaching of cerium to the reaction media. With only 0.9 mol% of mesoporous CeO_2@SiO_2 as main catalyst, the multicomponent condensation of aliphatic/aromatic aldehydes, 2-napthol and phenyl hydrazine with ethyl acetoacetate in water was induced to trigger a library of substituted pyrazolones in high yield and selectivity. The mechanism leading to the formation of substituted pyrazolones over CeO_2@SiO_2 is suggested to follow a sequential reaction of Knoevenagel condensation/Michael addition through two different pathways (Scheme 25.22).

25.2.4.3 CeO_2-Clay Composite

Another noticeable class of biomaterial is associated with hydroxyapatite [HAP; $Ca_{10}(PO_4)_6(OH)_2$] (Lu et al. 2019). This functional solid is highly recognized due to its outstanding properties such as high thermal stability, strong adsorption capability and tunable acidity/basicity (Pokhrel 2018). Accordingly, several investigations on the application of HAP as a solid catalyst or support in heterogeneous catalysis have been well executed (Fihri et al. 2017; Dobosz et al. 2016; Yan et al. 2016). In a typical study, Maddila et al. (2017b) doped ceria nanoparticles on hydroxyapatite (CeO_2@HAP) to induce the high-yielding assembly of pyrido[2,3-d]pyrimidine derivatives from the room-temperature coupling of benzaldehydes, dimethylbarbituric acid and ammonium acetate.

Honeycomb monolith (HM) is a type of solid material containing an extended matrix of long parallel and straight channels which are separated by thin walls (Govender and Friedrich 2017). This unique structural property generates a large number of void fractions and a large surface area to volume ratio. Furthermore, other major merits of honeycomb monolithic material encompass the high thermal conductivities, low pressure drops and ease of manufacturing and recyclability (Sungkono et al. 1997; Boger et al. 2004; Hosseini et al. 2020). Due to these reasons, HMs coated with metals/metal oxides are currently explored as heterogeneous catalysts in the NO_x reduction, N_2O decomposition, removal of SO_2-NO_x, syngas production, CO oxidation (Russo et al. 2007; Rico-Pérez et al. 2013; Vita et al. 2018a; Vita et al. 2018b; Davo-Quinonero et al. 2019) and organic synthesis (Gatica et al. 2016; Pratap et al. 2020). Recently, Venkatesh et al. (2015) prepared and applied the synthetic cordierite HM ($Mg_2Al_4Si_5O_{18}$) as a support to immobilize a set of cerium-based solid acids (i.e. sulphated CeO_2, CeO_2-ZrO_2 and sulphated CeO_2-ZrO_2) for the assembly of quinoxaline framework. It is disclosed that these cerium-based solid acids after coating with cordierite HM could display their supremacy over corresponding powder solid acids for the assembly of quinoxalines. In this

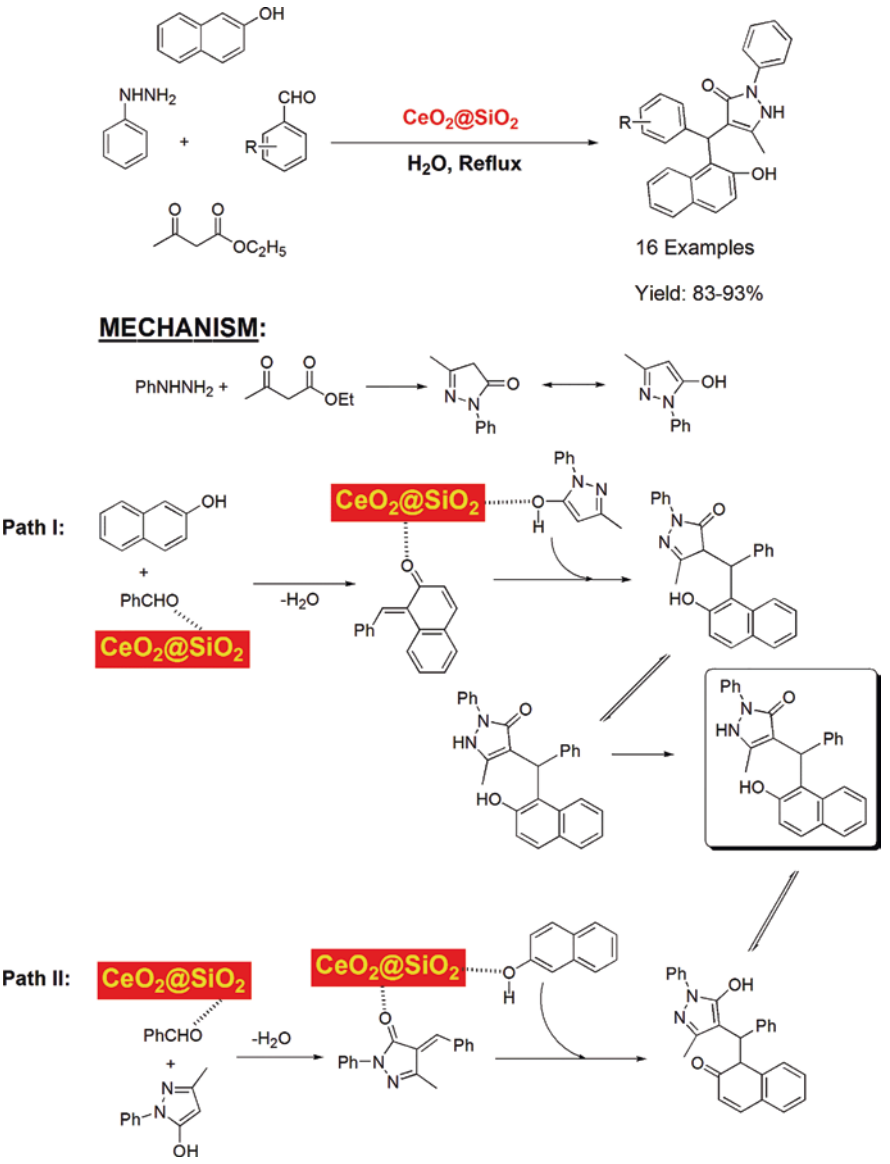

Scheme 25.22 Four-component assembly of substituted pyrazolones over CeO_2@SiO_2 nanocomposite

setting, high surface area, good dispersion of active sites and strong acidity of these acid-coated cordierites were acknowledged as main factors accounting for the high yield and selectivity of final products. Owing to high numbers of moderate and strong acid sites, HM-coated CeO_2-ZrO_2 was selected as the potential candidate for this synthetic paradigm, finally providing a group of quinoxalines in the range

yields of 72–89%. Strikingly, the spent catalyst could undergo six circulations with a negligible drop in the catalytic activity.

25.2.4.4 CeO_2-Carbon Template

Thanks to the unique properties (e.g. large surface area, excellent crystallinity, high physical/chemical/thermal stability and well-defined porosity), multi-walled carbon nanotubes (MWCNTs) have been exploited as versatile support in the fabrication of heterogeneous catalysts for the divergent synthesis of heterocycles (Safari and Gandomi-Ravandi 2014a, b, c; Zarnegar et al. 2015). By following this trend, Harikrishna et al. (2020) recently developed ceria-doped MWCNTs (CeO_2/MWCNTs) with 2.5 wt% of CeO_2 as a heterogeneous catalyst for the one-pot synthesis of pyridine-3-carboxamides. Under the promotion of recyclable CeO_2/MWCNTs nanocatalyst, the four-component coupling of acetoacetanilide, ammonium acetate and substituted aromatic aldehydes with ethyl cyanoacetate took place with no difficulty at room temperature. Accordingly, excellent isolated yields of pyridine-3-carboxamides (90–97%) could be delivered within a short period of time.

25.2.5 CeO_2 as Solid Support

In addition to being exploited as effective catalysts in the construction of diversified heterocyclic frameworks, several research groups also attempted to utilize the versatility of CeO_2 as a solid support to immobilize palladium metal (Pd@CeO_2) to facilitate the assembly of heterocycles (Scheme 25.23). For instance, Chen et al. (2014) reported the remarkable activity of Pd@CeO_2 in the oxidative synthesis of *N*-(2-pyridyl)indole derivatives. In this study, the Pd@CeO_2 was demonstrated to outperform other commercial catalysts (e.g. Rh@C, Ru@C and Pd@C) for this oxidative C-H activation. Unfortunately, the spent Pd@CeO_2 could not be recycled well, delivering a sharp drop in the yield of annulated products after two recycling tests. Later, Zhang et al. (2017) developed a facile one-pot redox strategy to fabricate self-assembled Pd/CeO_2 hybrid catalyst with 5.82 wt% of Pd, where the high-temperature stage of calcination and reduction was avoided in the pretreatment. Thanks to the high surface area and defect sites of CeO_2, the Pd/CeO_2 catalyst was able to trigger a quantitative yield of gamma-valerolactone (GVL) from the hydrogenation of levulinic acid (LA) under mild condition (90 °C, 4 bar of H_2), which showed the catalytic superiority over commercial Pd/C (yield: 7.5%) and conventional Pd/CeO_2 derived from the precipitation-reduction method (yield: 45.3%). In another case, Ge et al. (2018) applied Pd/CeO_2 (3 wt% Pd) as an effective nanophotocatalyst to trigger the photochemical synthesis of asymmetrical heterobiaryls.

With the aim of improving the isolated yields of benzimidazoylquinoxalines from current protocols, Climent et al. (2013) established an alternative synthetic pattern where the Au@CeO_2 with 2.33 wt% of Au was exploited as a potential

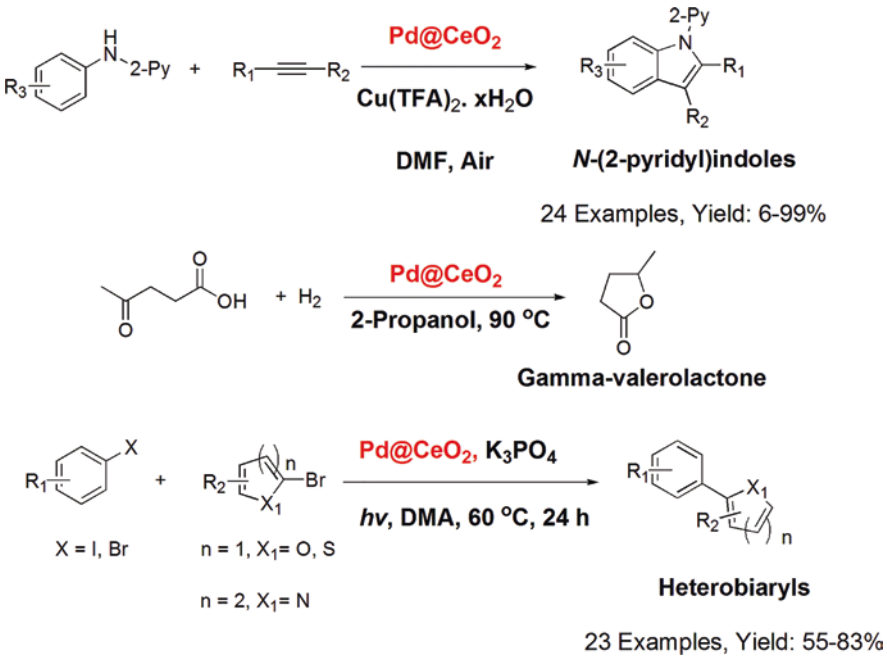

Scheme 25.23 Construction of various heterocyclic structures over Pd@CeO_2 nanocomposite

catalyst candidate. With the assistance of titled material, the trial for benzimidazoyl-quinoxalines could be attempted via two different manners (Scheme 25.24). In the straightforward approach, the oxidative coupling of the biomass-derived glycerol with 1,2-phenylene diamine was carried out in diglyme at 140 °C. In this case, two intermediates of quinoxalin-2-ylmethanol **A** and 1-(1H-benzo-[d]imidazol-2-yl) ethane-1,2-diol **B** were simultaneously generated from the coupling of 1,2-phenylene diamine with glyceraldehyde derived from the oxidation of glycerol. Afterwards, these intermediates would slowly undergo the oxidative condensation with 1,2-phenylene diamine to render the final 2-(1H-benzo[d]imidazol-2-yl)quinoxaline products (11 examples, yield: 24–80%). To expand the synthetic scope for constructing the benzimidazoylquinoxaline derivatives containing different substituents on both heteroaromatic moieties, the authors turned to deploy the one-pot two-step strategy upon starting with glyceraldehyde. In such case, 1-(1H-benzo-[d]imidazol-2-yl)ethane-1,2-diol **B** would be generated in water as the sole intermediate under the catalysis of Au@CeO_2 at room temperature, which was subsequently converted into a variety of substituted 2-(1H-benzo[d]imidazol-2-yl) quinoxaline upon oxidative coupling with substituted 1,2-phenylene diamines in diglyme at 140 °C (12 examples, yield: 63–79%). In each recycling trial, the recovered Au@CeO_2 was introduced to the calcination in O_2 at 250 °C prior to use, showing no significant loss in the original catalytic activity.

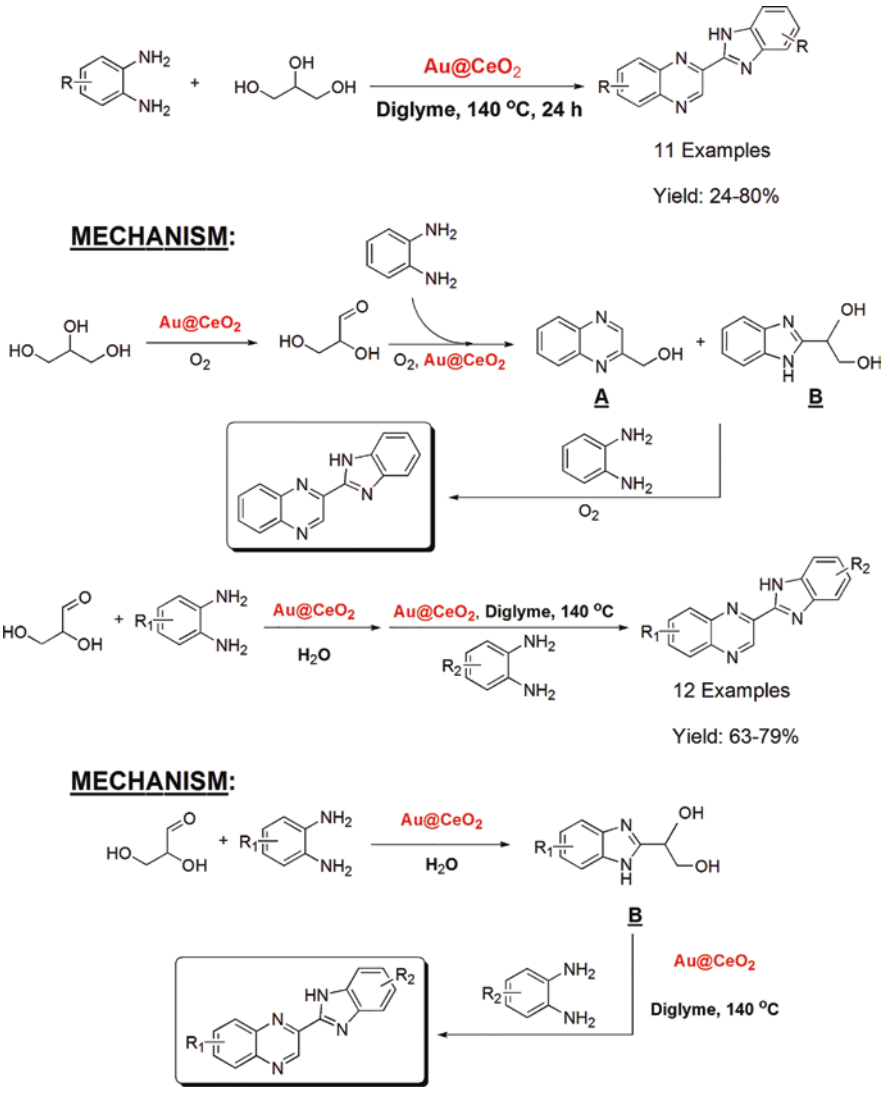

Scheme 25.24 Au@CeO_2-catalyzed synthesis of benzimidazoylquinoxalines

Furthermore, the practicality and efficiency of ceria-supported ruthenium (Ru@CeO_2) or ceria-supported platinum (Pt@CeO_2) as recyclable catalysts in the construction and functionalization of heterocycles such as indoles (Shimura et al. 2011), quinazolinones (An et al. 2018), ɣ-valerolactone (Gao et al. 2020), oxindoles (Chaudhari et al. 2014a) and quinazolines (Chaudhari et al. 2014b) have been realized in recent years (Scheme 25.25).

Another typical implementation of ceria-supported metal in the construction and functionalization of heteroarenes was introduced by Amadine et al. (2014), where

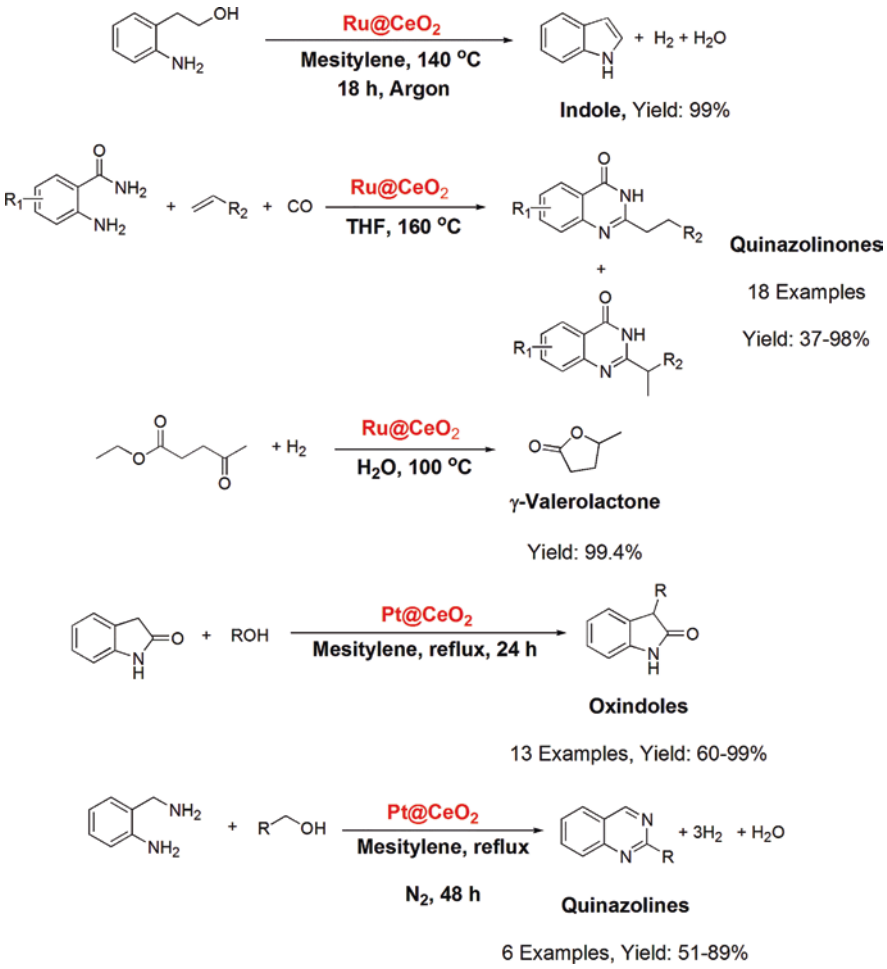

Scheme 25.25 Assembly of functionalized heterocycles over Ru@CeO_2 and Pt/CeO_2 catalyst

the ceria-supported copper nanoparticles (Cu@CeO_2) displayed the excellent catalytic activity in the *N*-arylation of indole with various aryl bromides. Although 82–89% isolated yields of *N*-arylated indoles could be achieved under optimal conditions, a considerable drop in the activity of spent Cu@CeO_2 was observed after three cycles. In this context, the reasons were likely attributed to the unavoidable oxidation of Cu^0 to Cu^{2+} and the poisonous deposition of in situ generated KBr on the surface of Cu@CeO_2. Later, Amini et al. (2016) reported the utility of robust Cu@CeO_2 nanocomposite (10 wt% Cu) to formulate a collection of 1,2,3-triazole derivatives (yield: 62–96%) from the 1,3-dipolar cycloaddition of terminal alkynes with sodium azide and benzyl halide derivatives in water.

25.3 Cerium-Based Catalysts for the Vapour-Phase Synthesis of Heterocycles

Recently, the catalysis of ceria-supported metal oxides for the vapour-phase synthesis of γ-butyrolactone (GBL) has been investigated due to the great importance and high output demand of GBL in industry (Schwarz et al. 2019). For example, Bhanushali et al. (2019) introduced the ceria supported copper ($CuO@CeO_2$) with 10 wt.% of Cu as an effective catalyst for the fixed-bed dehydrogenation of 1,4-butanediol (1,4-BDO) at 240 °C. Thanks to the high surface area, good dispersion of cooper on the ceria support and an enhancement in basicity, the $CuO@CeO_2$ could induce the dehydrogenation in an effective manner to trigger 93% conversion of 1,4-BDO and 98% selectivity of GBL. Subsequently, 10 wt% of Cu supported on CeO_2-Al_2O_3 (3:1 ratio) catalyst was able to promote the one-pot synthesis of GBL and benzyl alcohol from the simultaneous 1,4-BDO dehydrogenation and benzaldehyde hydrogenation, in which 90% conversion of 1,4-BDO and 95% selectivity of GBL were accomplished (Bhanushali et al. 2020a). Lately, 99% yield and 99% selectivity of GBL from the direct dehydrogenation of 1,4-BDO at 240 °C could be reachable in the presence of mesoporous 10 wt% $CuO@CeO_2$-Al_2O_3 (3:1 ratio) (Bhanushali et al. 2020b). In these examples, a remarkable decrease in conversion of 1,4-BDO up to 45% was unavoidable due to the coke deposition and agglomeration of copper nanoparticles after a long-time span on stream at high temperature.

Thanks to the high atom-economic, low cost and benign aspects, the vapour-phase synthesis of 3-methylindole from glycerol and aniline has drawn much interest over the past few years. In such transformation, the heterogeneous catalysts containing a large specific area along with a great number of weak acidic sites are strongly required to offer high yield and selectivity of the target product (Sun et al. 2010; Cui et al. 2013). Recently, Ke et al. (2020) applied the Cu/MIL-101 modified with CeO_2 (0.03 mmol/g) to prepare 59% yield of 3-methylindole from this synthetic paradigm. In this study, the authors stated that the addition of CeO_2 was conducive to the catalytic activity for the sake of (i) enhancing the mutual interaction of Cu and MIL-101; (ii) inhibiting the sintering of active components during the transformation; and (iii) increasing the number of weak acid sites on the surface of catalyst. Later, Qu et al. (2020) successfully fabricated mesoporous catalyst of Ag/SBA-15 modified with ZnO-CeO_2 (1 mmol/g of Ag, 1 mmol/g of ZnO and 0.05 mmol/g of CeO_2) to upgrade the yield of 3-methylindole up to 62%.

25.4 Cerium-Based Catalysts for the Synthesis of CO_2-Derived Heterocycles

Apart from being employed as heterogeneous catalysts in the manufacture of CO_2-based products such as ureas (Tamura et al. 2016a), carbamates (Tomishige et al. 2019), carbonates (Tomishige et al. 2020) and polycarbonates (Gu et al. 2019;

Tamura et al. 2016b), cerium-based materials have been widely applied in the catalytic fixation of CO_2 towards heterocycles as well. For example, Tamura et al. (2013a) established a novel catalyst system composed of CeO_2 and 2-propanol to promote the synthesis of cyclic ureas from CO_2 and diamines. In this study, it is revealed that the presence of 2-propanol was essential to suppress the competitive formation of *N*-alkylated amines. Through the kinetic and FTIR investigations, the CeO_2-mediated cyclization is proposed to follow a cascade reaction of (i) simultaneous adsorption of diamine with CO_2 and CeO_2 to generate carbamic acid and carbamate adspecies on ceria; (ii) decomposition of carbamate species to a free amino group; (iii) annulation to cyclic urea by the intramolecular attack of amino group to the activated carbamate part; and (iv) desorption of the cyclic urea product and regeneration of CeO_2 (Scheme 25.26).

For the manufacture of CO_2-based cyclic carbonates such as ethylene carbonate (EC) and propylene carbonate (PC), Tomishige et al. (2004) reported the coupling pattern of ethylene glycol (EG) or propylene glycol (PG) with CO_2 over $Ce_xZr_{1-x}O_2$ solid solution. The authors stated that the acetonitrile as solvent helped to improve the catalytic activity and the equilibrium yield of carbonates in this reaction. Additionally, the maximal yield of both EC and PC could be obtained with CeO_2–ZrO_2 (Ce/[Ce+Zr] = 0.5) calcined at 800 °C or CeO_2–ZrO_2 (Ce/[Ce+Zr] = 0.2 and 0.33) calcined at 1000 °C. Later, Honda et al. (2014) examined the convenience of CeO_2 for the approach to five-/six-membered cyclic carbonates from diols and CO_2. It is verified that the introduction of excessive 2-cyanopyridine (2-CP) as a dehydrating agent was indispensable to overcome the equilibrium limitation, where the in situ generated water was effectively trapped by 2-CP. In the mechanistic description (Scheme 25.27), CeO_2 served as a Lewis acid to deprotonate the O-H bond of diol, thereby generating the cerium alkoxide **I** at the first stage. Afterwards, this alkoxide would allow the insertion of CO_2 to form the carbonate specie **II**, followed by the intramolecular cyclization and dehydration to result in the final cyclic carbonate.

In the production of glycerol carbonate, Liu et al. (2016) carried out the CeO_2-mediated carbonylation of glycerol with CO_2 in the presence of DMF and dehydrating agent (2-cyanopyridine). For this purpose, the authors attempted three types of CeO_2 derived from the traditional precipitation (TP), hydrothermal (HT) and citrate sol-gel (SG) method for the CO_2 carbonylation. From the CO_2-TPD and H_2-TPR analysis, the basicity and oxygen vacancy density of these designed CeO_2 followed the order of nano-rod CeO_2 (HT) > nanoparticulate CeO_2 (TP) > sponge-like CeO_2 (SG). Hence, the highest yield of glycerol carbonate (78.9%) was provided under the mediation of nano-rod CeO_2 upon heating glycerol with CO_2 at 150 °C. By following the same strategy, Liu et al. (2018) applied the $Ce_{098}Zr_{002}O_2$ derived from the hydrothermal method to deliver 36.3% yield of glycerol carbonate.

To investigate the conversion of CO_2 into 2-oxazolidinones, Juarez et al. (2010) examined CeO_2 NP (5 nm) and commercial CeO_2 (40 nm) to promote the coupling of CO_2 and ω-aminoalcohols. Due to the high density of defects on the surface, the CeO_2 NPs (5 nm) displayed the best results in converting CO_2, and *N*-alkyl substituted aminoethanols into corresponding *N*-alkyl 1,3-oxazolidin-2-ones at

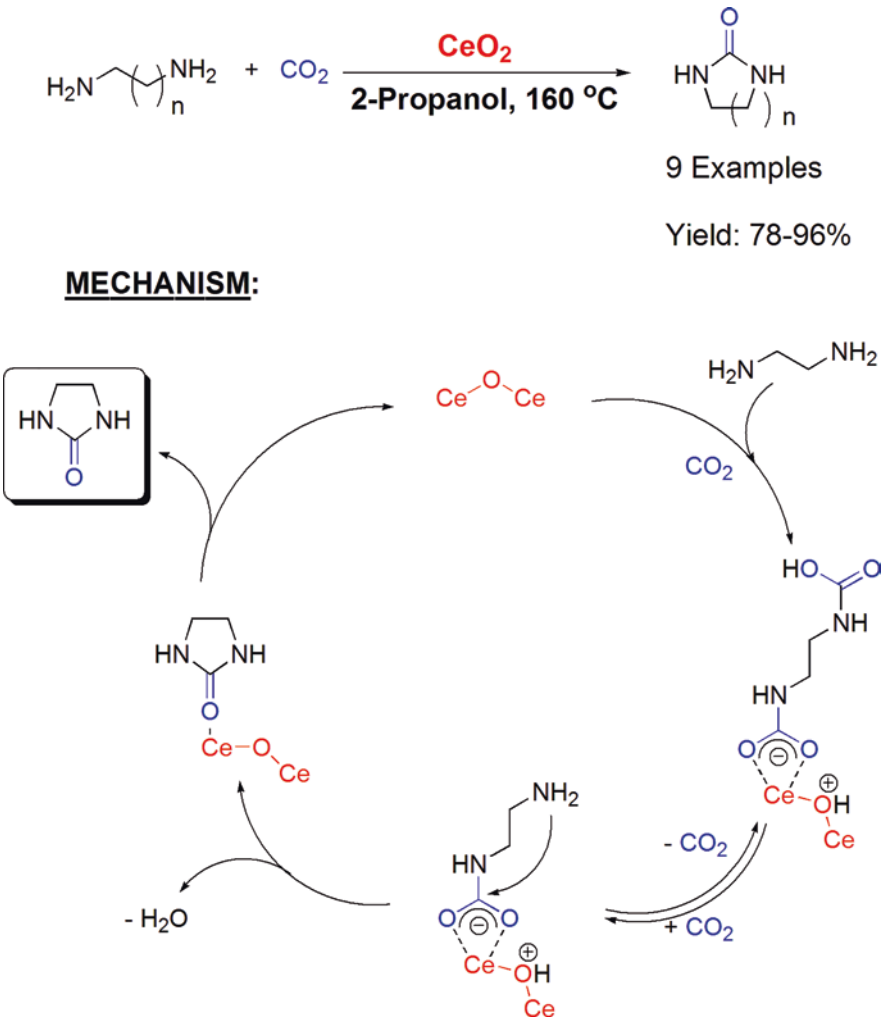

Scheme 25.26 Synthesis of cyclic ureas from CO_2 and diamines over CeO_2 in 2-propanol

160 °C. Later, Tamura et al. (2013b) stated that a variety of aminoalcohols could be selectively converted into corresponding cyclic carbamates in high yields (88–99%) over the catalytic system of CH_3CN-CeO_2. In particular, the chiral configuration of chiral centre at the α-position of the hydroxyl group of starting aminoalcohols was kept intact after the reaction. From the kinetic studies and FTIR analyses, the mechanistic pathway leading to the generation of 2-oxazolidinones over CeO_2 is suggested to follow four consecutive steps as shown in Scheme 25.28.

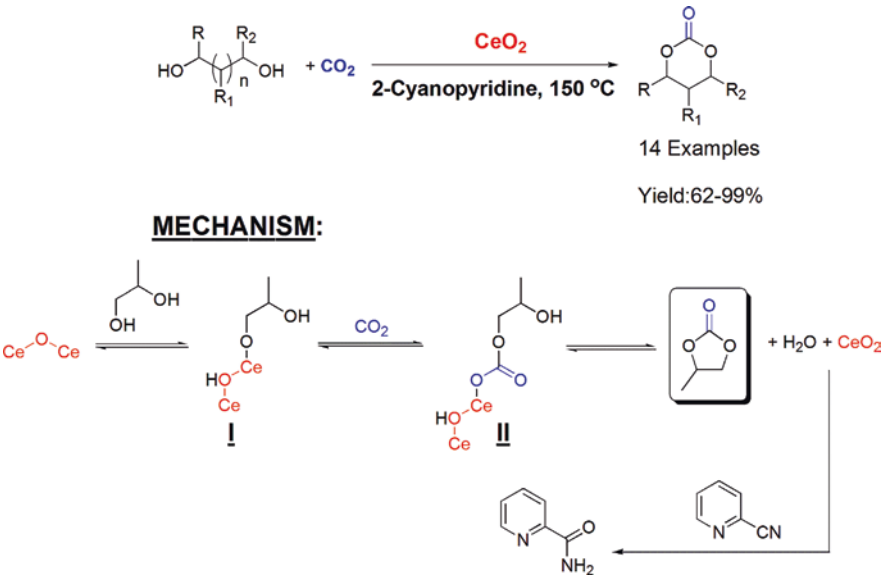

Scheme 25.27 Synthesis of cyclic carbonates from CO_2 and diols under the catalysis of CeO_2 and 2-cyanopyridine

25.5 Summary and Outlook

The great importance and omnipresence of heterocyclic frameworks in natural products, bioactive molecules, pharmaceuticals and key building blocks have continuously raised the interest in developing novel, eco-friendly and sustainable protocols to improve the time/energy consumption, atom economy and selectivity during the manufacture. In this chapter, the broad practicality of cerium-based nanomaterials as both catalysts and solid supports in the synthesis and functionalization of heterocycles was summarized, where a diversity of heterocyclic skeletons containing nitrogen, oxygen and/or sulphur atom was constructed successfully under heterogeneous conditions. For this objective, well-defined cerium-based materials such as cerium oxide/mixed oxides, cerium composites and ceria-supported metals were fabricated over different procedures including co-precipitation, sol-gel, hydrothermal, wet impregnation and so on. With tunable modifications of morphology, acidity-basicity, redox properties and oxygen storage capacity, these nanocatalysts turned out to be potential heterogeneous candidates for the divergent synthesis of heterocyclic compounds. Particularly, their excellent catalytic performances were also recognized in the chemical fixation of CO_2, where valuable cyclic products of ureas, carbonates and carbamates were accomplished in great success. In such transformations, cheap, robust, easy-to-handle and recoverable nature are noticeable merits of these cerium-based nanomaterials in comparison with other benchmark catalysts. However, further improvements in this synthetic

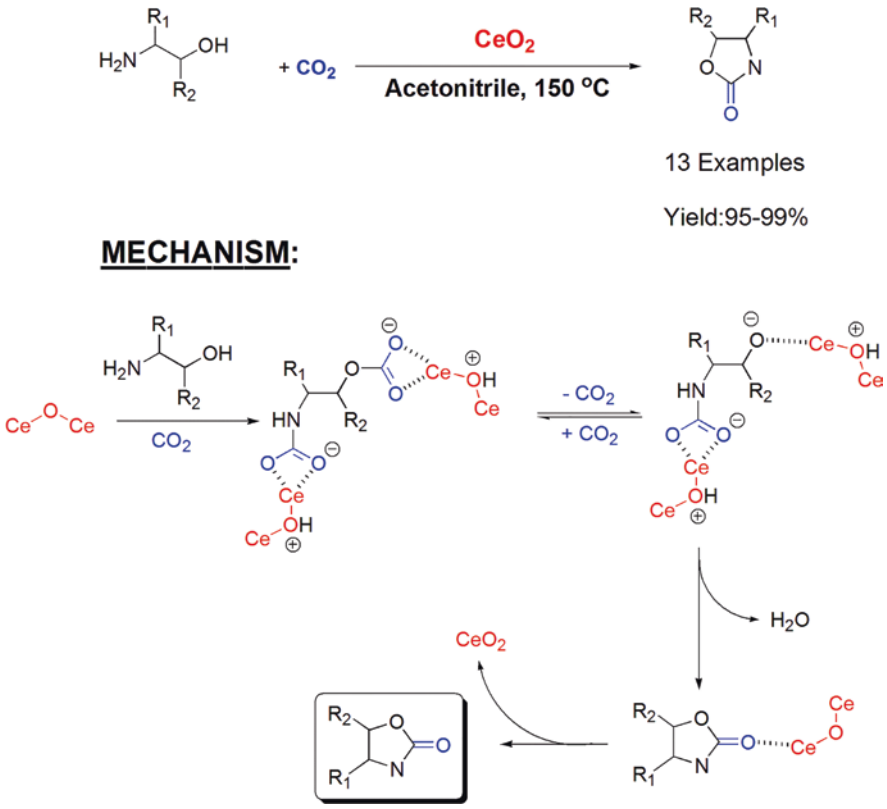

Scheme 25.28 CeO_2-mediated coupling of CO_2 and aminoalcohols towards *N*-alkyl 1,3-oxazolidin-2-ones

strategy need to be carried out, where the development of simple, cheap and effective processes for the fabrication of cerium-based nanomaterials is strongly desired. In this manner, utilizing the latest advent of nanotechnology in controlling the size, shape and composition of final cerium oxide/mixed oxides is considered of great importance to maximize the number and strength of active sites for specific reactions. Moreover, the architecture of the solid supports and their interaction with cerium nanoparticles need to be carefully considered as well. In another aspect, the catalysis of cerium-based nanostructures in the MCR patterns should be further explored to expand the molecular complexity of heterocyclic frameworks. Last but not least, solvent-free or aqueous-phase paradigms are highly appreciated for the eco-friendly and sustainable synthesis of heterocycles.

References

Agotegaray MA, Lassalle VL (2017) Silica: chemical properties and biological features. In: Silica-coated magnetic nanoparticles. Springer, Cham, pp 27–37

Akbayrak S (2018) Rhodium(0) nanoparticles supported on ceria as catalysts in hydrogenation of neat benzene at room temperature. J Colloid Interface Sci 530:459–464

Akelah A (1981) Use of functionalised silica in catalysis and organic synthesis. Br Polym J 13:107–110

Akondi AM, Trivedi R, Sreedhar B, Kantam ML, Bhargava S (2012) Cerium-containing MCM-41 catalyst for selective oxidative arene cross-dehydrogenative coupling reactions. Catal Today 198:35–44

Akondi AM, Kantam ML, Trivedi R, Sreedhar B, Buddana SK, Prakasham RS, Bhargava S (2014) Formation of benzoxanthenones and benzochromenones via cerium-impregnated-MCM-41 catalyzed, solvent-free, three-component reaction and their biological evaluation as antimicrobial agents. J Mol Catal A Chem 386:49–60

Akondi AM, Kantam ML, Trivedi R, Bharatam J, Vemulapalli SPB, Bhargava SK, Buddana SK, Prakasham RS (2016) Ce/SiO2 composite as an efficient catalyst for the multicomponent one-pot synthesis of substituted pyrazolones in aqueous media and their antimicrobial activities. J Mol Catal A Chem 411:325–336

Albadi J, Razeghi A, Abbaszadeh H, Mansournezhad A (2013a) CuO-CeO2 nanocomposite: an efficient recyclable catalyst for the synthesis of Aryl-14H-dibenzo[a-j]xanthenes. J Nanoparticles 2013:1–5

Albadi J, Mansournezhad A, Abbaszadeh H (2013b) CuO-CeO2Nanocomposite: a highly efficient recyclable catalyst for the green synthesis of 1,8-Dioxooctahydroxanthenes in water. J Chin Chem Soc:n/a–n/a

Albadi J, Mansournezhad A, Derakhshandeh Z (2013c) CuO–CeO2 nanocomposite: a highly efficient recyclable catalyst for the multicomponent synthesis of 4H-benzo[b]pyran derivatives. Chin Chem Lett 24:821–824

Albadi J, Razeghi A, Mansournezhad A, Azarian Z (2013d) CuO-CeO2 nanocomposite catalyzed efficient synthesis of aminochromenes. J Nanostruct Chem 3:85

Albadi J, Mansournezhad A, Salehnasab S (2014a) Green synthesis of biscoumarin derivatives catalyzed by recyclable CuO–CeO2 nanocomposite catalyst in water. Res Chem Intermed 41:5713–5721

Albadi J, Shiran JA, Mansournezhad A (2014b) Click synthesis of 1,4-disubstituted-1,2,3-triazoles catalysed by CuO–CeO2 nanocomposite in the presence of amberlite-supported azide. J Chem Sci 126:147–150

Ali I, Lone MN, Al-Othman ZA, Al-Warthan A, Sanagi MM (2015) Heterocyclic Scaffolds: centrality in anticancer drug development. Curr Drug Targets 16:711–734

Amadine O, Maati H, Abdelouhadi K, Fihri A, El Kazzouli S, Len C, El Bouari A, Solhy A (2014) Ceria-supported copper nanoparticles: a highly efficient and recyclable catalyst for N-arylation of indole. J Mol Catal A Chem 395:409–419

Amini M, Hassandoost R, Bagherzadeh M, Gautam S, Chae KH (2016) Copper nanoparticles supported on CeO2 as an efficient catalyst for click reactions of azides with alkynes. Catal Commun 85:13–16

An J, Wang Y, Zhang Z, Zhao Z, Zhang J, Wang F (2018) The synthesis of Quinazolinones from Olefins, CO, and Amines over a heterogeneous Ru-clusters/Ceria catalyst. Angew Chem Int Ed Engl 57:12308–12312

Arumugam A, Karthikeyan C, Haja Hameed AS, Gopinath K, Gowri S, Karthika V (2015) Synthesis of cerium oxide nanoparticles using Gloriosa superba L. leaf extract and their structural, optical and antibacterial properties. Mater Sci Eng C Mater Biol Appl 49:408–415

Arya A, Sethy NK, Das M, Singh SK, Das A, Ujjain SK, Sharma RK, Sharma M, Bhargava K (2014) Cerium oxide nanoparticles prevent apoptosis in primary cortical culture by stabilizing mitochondrial membrane potential. Free Radic Res 48:784–793

Babu CM, Vinodh R, Abidov A, Ravikumar R, Peng MM, Cha WS, Jang HT (2016) Caprolactam synthesis using Ce-MCM-41Catalysts. Int J Bio-Sci Bio-Technol 8:171–182

Baumann M, Baxendale IR (2013) An overview of the synthetic routes to the best selling drugs containing 6-membered heterocycles. Beilstein J Org Chem 9:2265–2319

Baumann M, Baxendale IR, Ley SV, Nikbin N (2011) An overview of the key routes to the best selling 5-membered ring heterocyclic pharmaceuticals. Beilstein J Org Chem 7:442–495

Bhanushali JT, Prasad D, Patil KN, Babu GVR, Kainthla I, Rao KSR, Jadhav AH, Nagaraja BM (2019) The selectively regulated vapour phase dehydrogenation of 1,4-butanediol to γ-butyrolactone employing a copper-based ceria catalyst. New J Chem 43:11968–11983

Bhanushali JT, Prasad D, Patil KN, Reddy KS, Rama Rao KS, Jadhav AH, Nagaraja BM (2020a) Simultaneous dehydrogenation of 1,4- butanediol to γ-butyrolactone and hydrogenation of benzaldehyde to benzyl alcohol mediated over competent CeO2–Al2O3 supported Cu as catalyst. Int J Hydrog Energy 45:12874–12888

Bhanushali JT, Prasad D, Patil KN, Reddy KS, Kainthla I, Rao KSR, Jadhav AH, Nagaraja BM (2020b) Tailoring the catalytic activity of basic mesoporous cu/CeO2 catalyst by Al2O3 for selective lactonization and dehydrogenation of 1,4-butanediol to γ-butyrolactone. Catal Commun 143:106049

Bhattacharyya S, Lelong G, Saboungi ML (2006) Recent progress in the synthesis and selected applications of MCM-41: a short review. J Exp Nanosci 1:375–395

Boger T, Heibel AK, Sorensen CM (2004) Monolithic catalysts for the chemical industry. Ind Eng Chem Res 43:4602–4611

Bumajdad A, Zaki MI, Eastoe J, Pasupulety L (2004) Microemulsion-based synthesis of CeO(2) powders with high surface area and high-temperature stabilities. Langmuir 20:11223–11233

Burange AS, Gawande MB (2016) Role of mixed metal oxides in heterogeneous catalysis. In: Encyclopedia of inorganic and bioinorganic chemistry. Wiley, Hoboken, pp 1–19

Cargnello M, Jaen JJD, Garrido JCH, Bakhmutsky K, Montini T, Gamez JJC, Gorte RJ, Fornasiero P (2012) Exceptional activity for methane combustion over modular Pd@CeO2 subunits on functionalized Al2O3. Science 337:713–717

Carson CA, Kerr MA (2009) Heterocycles from cyclopropanes: applications in natural product synthesis. Chem Soc Rev 38:3051–3060

Chang K, Zhang H, Cheng M-j, Lu Q (2019) Application of Ceria in CO2 conversion catalysis. ACS Catal 10:613–631

Channei D, Inceesungvorn B, Wetchakun N, Ukritnukun S, Nattestad A, Chen J, Phanichphant S (2014) Photocatalytic degradation of methyl orange by CeO2 and Fe–doped CeO2 films under visible light irradiation. Sci Rep 4:5757

Chaudhari C, Siddiki SMAH, Kon K, Tomita A, Tai Y, Shimizu K-i (2014a) C-3 alkylation of oxindole with alcohols by Pt/CeO2 catalyst in additive-free conditions. Cat Sci Technol 4:1064–1069

Chaudhari C, Hakim Siddiki SMA, Tamura M, Shimizu K-i (2014b) Acceptorless dehydrogenative synthesis of 2-substituted quinazolines from 2-aminobenzylamine with primary alcohols or aldehydes by heterogeneous Pt catalysts. RSC Adv 4:53374–53379

Chen H-I, Chang H-Y (2005) Synthesis of nanocrystalline cerium oxide particles by the precipitation method. Ceram Int 31:795–802

Chen P-L, Chen IW (1993) Reactive cerium(IV) oxide powders by the homogeneous precipitation method. J Am Ceram Soc 76:1577–1583

Chen J, He L, Natte K, Neumann H, Beller M, Wu X-F (2014) Palladium@Cerium(IV) oxide-catalyzed oxidative synthesis of N-(2-Pyridyl)indoles via C–H activation reaction. Adv Synth Catal 356:2955–2959

Climent MJ, Corma A, Iborra S, Martínez-Silvestre S (2013) Gold catalysis opens up a new route for the synthesis of Benzimidazoylquinoxaline derivatives from biomass-derived products (glycerol). ChemCatChem 5:3866–3874

Colussi S, Gayen A, Farnesi Camellone M, Boaro M, Llorca J, Fabris S, Trovarelli A (2009) Nanofaceted Pd–O sites in Pd–Ce surface superstructures: enhanced activity in catalytic combustion of methane. Angew Chem Int Ed 48:8481–8484

Courty P, Marcilly C (1976) General synthesis methods for mixed oxide catalysts. In: Studies in surface science and catalysis, vol 1. Elsevier, Amsterdam, pp 119–145

Cousin P, Ross RA (1990) Preparation of mixed oxides: a review. Mater Sci Eng A 130:119–125

Cui Y, Zhou X, Sun Q, Shi L (2013) Vapor-phase synthesis of 3-methylindole from glycerol and aniline over zeolites-supported Cu-based catalysts. J Mol Catal A Chem 378:238–245

D'Alessandro O, Sathicq ÁG, Sambeth JE, Thomas HJ, Romanelli GP (2015) A study of the temperature effect on Hantzsch reaction selectivity using Mn and Ce oxides under solvent-free conditions. Catal Commun 60:65–69

Darroudi M, Hoseini SJ, Kazemi Oskuee R, Hosseini HA, Gholami L, Gerayli S (2014) Food-directed synthesis of cerium oxide nanoparticles and their neurotoxicity effects. Ceram Int 40:7425–7430

Davo-Quinonero A, Sorolla-Rosario D, Bailon-Garcia E, Lozano-Castello D, Bueno-Lopez A (2019) Improved asymmetrical honeycomb monolith catalyst prepared using a 3D printed template. J Hazard Mater 368:638–643

Delost MD, Smith DT, Anderson BJ, Njardarson JT (2018) From Oxiranes to oligomers: architectures of U.S. FDA approved pharmaceuticals containing oxygen heterocycles. J Med Chem 61:10996–11020

Deshpande SS, Sonavane SU, Jayaram RV (2008) A facile deprotection of oximes over mixed metal oxides under solvent-free conditions. Catal Commun 9:639–644

Dey S, Dhal GC (2020) Ceria doped CuMnOx as carbon monoxide oxidation catalysts: synthesis and their characterization. Surfaces Interfaces 18:100456

Do J, Chava R, Son N, Kim J, Park N-K, Lee D, Seo M, Ryu H-J, Chi J, Kang M (2018) Effect of Ce doping of a Co/Al2O3 catalyst on hydrogen production via propane steam reforming. Catalysts 8:413

Dobosz J, Hull S, Zawadzki M (2016) Catalytic activity of cobalt and cerium catalysts supported on calcium hydroxyapatite in ethanol steam reforming. Pol J Chem Technol 18:59–67

Du N, Zhang H, Chen B, Ma X, Yang D (2007) Ligand-free self-assembly of Ceria nanocrystals into nanorods by oriented attachment at low temperature. J Phys Chem C 111:12677–12680

Edayadulla N, Lee YR (2014) Cerium oxide nanoparticle-catalyzed three-component protocol for the synthesis of highly substituted novel quinoxalin-2-amine derivatives and 3,4-dihydroquinoxalin-2-amines in water. RSC Adv 4:11459

Esposito S (2019) "Traditional" Sol-Gel chemistry as a powerful tool for the preparation of supported metal and metal oxide catalysts. Materials (Basel) 12:668

Fayaz F, Danh HT, Nguyen-Huy C, Vu KB, Abdullah B, Vo D-VN (2016) Promotional effect of Ce-dopant on Al2O3-supported Co catalysts for syngas production via CO2 reforming of ethanol. Proc Eng 148:646–653

Feng M, Tang B, Liang SH, Jiang X (2016) Sulfur containing scaffolds in drugs: synthesis and application in medicinal chemistry. Curr Top Med Chem 16:1200–1216

Ferreira NS, Angélica RS, Marques VB, de Lima CCO, Silva MS (2016) Cassava-starch-assisted sol–gel synthesis of CeO 2 nanoparticles. Mater Lett 165:139–142

Fihri A, Len C, Varma RS, Solhy A (2017) Hydroxyapatite: a review of syntheses, structure and applications in heterogeneous catalysis. Coord Chem Rev 347:48–76

Fiorenza R, Bellardita M, D'Urso L, Compagnini G, Palmisano L, Scirè S (2016) Au/TiO2-CeO2 catalysts for photocatalytic water splitting and VOCs oxidation reactions. Catalysts 6:121

Fu J, Liu N, Mei L, Liao L, Deyneko D, Wang J, Bai Y, Lv G (2019) Synthesis of Ce-doped Mn3Gd7-xCex(SiO4)6O1.5 for the enhanced catalytic ozonation of tetracycline. Sci Rep 9:18734

Gadipelly C, Mannepalli LK (2019) Nano-metal oxides for organic transformations. Curr Opin Green Sustain Chem 15:20–26

Gao X, Zhu S, Dong M, Wang J, Fan W (2020) Ru/CeO2 catalyst with optimized CeO2 morphology and surface facet for efficient hydrogenation of ethyl levulinate to γ-valerolactone. J Catal 389:60–70

Gatica JM, García-Cabeza AL, Yeste MP, Marín-Barrios R, González-Leal JM, Blanco G, Cifredo GA, Guerra FM, Vidal H (2016) Carbon integral honeycomb monoliths as support of copper catalysts in the Kharasch–Sosnovsky oxidation of cyclohexene. Chem Eng J 290:174–184

Gawande MB, Pandey RK, Jayaram RV (2012) Role of mixed metal oxides in catalysis science—versatile applications in organic synthesis. Cat Sci Technol 2:1113

Gawande MB, Branco PS, Varma RS (2013a) Nano-magnetite (Fe3O4) as a support for recyclable catalysts in the development of sustainable methodologies. Chem Soc Rev 42:3371–3393

Gawande MB, Bonifácio VDB, Varma RS, Nogueira ID, Bundaleski N, Ghumman CAA, Teodoro OMND, Branco PS (2013b) Magnetically recyclable magnetite–ceria (Nanocat-Fe-Ce) nanocatalyst – applications in multicomponent reactions under benign conditions. Green Chem 15:1226

Ge Y, Diao P, Xu C, Zhang N, Guo C (2018) Visible light induced cross-coupling synthesis of asymmetrical heterobiaryls using Pd/CeO2 nanocomposite photocatalyst. Chin Chem Lett 29:903–906

Gharib A, Hashemipour Khorasani BR, Jahangir M, Roshani M, Safaee R (2013) Catalytic synthesis of 3-Methyl-1-phenyl-1H-benzo[g]pyrazolo[3,4-b]quinoline-5,10-dione derivatives using cerium oxide nanoparticles as heterogeneous catalyst in green conditions. Organic Chem Int 2013:1–5

Ghayour F, Mohammad Shafiee MR, Ghashang M (2018) ZnO-CeO2 nanocomposite: efficient catalyst for the preparation of thieno[2,3-d]pyrimidin-4(3H)-one derivatives. Main Group Metal Chem 41:1

Girija DK, Naik H, Sudhamani C, Kumar BV (2011) Cerium oxide nanoparticles-a green, reusable, and highly efficient heterogeneous catalyst for the synthesis of Polyhydroquinolines under solvent-free conditions. Arch Appl Sci Res 3:373

Gomtsyan A (2012) Heterocycles in drugs and drug discovery. Chem Heterocycl Compd 48:7–10

Gopinath K, Karthika V, Sundaravadivelan C, Gowri S, Arumugam A (2015) Mycogenesis of cerium oxide nanoparticles using Aspergillus niger culture filtrate and their applications for antibacterial and larvicidal activities. J Nanostruct Chem 5:295–303

Govender S, Friedrich H (2017) Monoliths: a review of the basics, preparation methods and their relevance to oxidation. Catalysts 7:62

Grzybowska-Swierkosz B (1987) Acidic properties of mixed transition metal oxides. Mater Chem Phys 17:121–144

Gu Y, Matsuda K, Nakayama A, Tamura M, Nakagawa Y, Tomishige K (2019) Direct synthesis of alternating polycarbonates from CO2 and diols by using a catalyst system of CeO2 and 2-Furonitrile. ACS Sustain Chem Eng 7:6304–6315

Guo Z, Liu B, Zhang Q, Deng W, Wang Y, Yang Y (2014) Recent advances in heterogeneous selective oxidation catalysis for sustainable chemistry. Chem Soc Rev 43:3480–3524

Guo T, Yao M-S, Lin Y-H, Nan C-W (2015) A comprehensive review on synthesis methods for transition-metal oxide nanostructures. CrystEngComm 17:3551–3585

Harikrishna S, Robert AR, Ganja H, Maddila S, Jonnalagadda SB (2020) A green, efficient and recoverable CeO2/MWCNT nanocomposite catalyzed click synthesis of pyridine-3-carboxamides. Appl Organomet Chem 34:e5796

Honda M, Tamura M, Nakao K, Suzuki K, Nakagawa Y, Tomishige K (2014) Direct cyclic carbonate synthesis from CO2 and Diol over carboxylation/hydration cascade catalyst of CeO2 with 2-Cyanopyridine. ACS Catal 4:1893–1896

Hosseini S, Moghaddas H, Masoudi Soltani S, Kheawhom S (2020) Technological applications of Honeycomb Monoliths in environmental processes: a review. Process Saf Environ Prot 133:286–300

Hu Z, Tan S, Mi R, Li X, Li D, Yang B (2018) Solvent-controlled reactivity of Au/CeO2 towards hydrogenation of p-Chloronitrobenzene. Catal Lett 148:1490–1498

Huang W, Gao Y (2014) Morphology-dependent surface chemistry and catalysis of CeO2nanocrystals. Cat Sci Technol 4:3772–3784

Juarez R, Concepcion P, Corma A, Garcia H (2010) Ceria nanoparticles as heterogeneous catalyst for CO2 fixation by omega-aminoalcohols. Chem Commun (Camb) 46:4181–4183

Kamruddin M, Ajikumar PK, Nithya R, Tyagi AK, Raj B (2004) Synthesis of nanocrystalline ceria by thermal decomposition and soft-chemistry methods. Scr Mater 50:417–422

Kargar H, Ghazavi H, Darroudi M (2015) Size-controlled and bio-directed synthesis of ceria nanopowders and their in vitro cytotoxicity effects. Ceram Int 41:4123–4128

Ke K, Wu F, Ren L, Jiao Y, Xing N, Shi L (2020) An efficient catalyst of Cu/MIL-101 modified with CeO2 for the conversion of biomass-derived glycerol with aniline to 3-methylindole. Catal Commun 136:105896

Khan S, Agasar M, Ghosh A, Keri RS (2019) A novel, multi-component method of preparation of Quinolines using recyclable CeO2-TiO2 nanocomposite catalyst under solvent-free conditions. Org Prep Proced Int 51:153–160

Korotkova AM, Borisovna PO, Aleksandrovna GI, Bagdasarovna KD, Vladimirovich BD, Vladimirovich KD, Alexandrovich FA, Yurievna KM, Nikolaevna BE, Aleksandrovich KD, Yurievich CM, Valerievich LS (2019) "Green" synthesis of cerium oxide particles in water extracts Petroselinum crispum. Curr Nanomater 4:176–190

Kumar PSV, Suresh L, Vinodkumar T, Reddy BM, Chandramouli GVP (2016) Zirconium doped Ceria nanoparticles: an efficient and reusable catalyst for a green multicomponent synthesis of novel Phenyldiazenyl–Chromene derivatives using aqueous medium. ACS Sustain Chem Eng 4:2376–2386

Laberty-Robert C, Long JW, Lucas EM, Pettigrew KA, Stroud RM, Doescher MS, Rolison DR (2006) Sol−gel-derived Ceria nanoarchitectures: synthesis, characterization, and electrical properties. Chem Mater 18:50–58

Lamberth C (2013) Heterocyclic chemistry in crop protection. Pest Manag Sci 69:1106–1114

Liang J, Liang Z, Zou R, Zhao Y (2017) Heterogeneous catalysis in Zeolites, Mesoporous Silica, and metal-organic frameworks. Adv Mater 29

Liu J, Li Y, Zhang J, He D (2016) Glycerol carbonylation with CO2 to glycerol carbonate over CeO2 catalyst and the influence of CeO2 preparation methods and reaction parameters. Appl Catal A Gen 513:9–18

Liu J, Li Y, Liu H, He D (2018) Transformation of CO2 and glycerol to glycerol carbonate over CeO2ZrO2 solid solution —— effect of Zr doping. Biomass Bioenergy 118:74–83

Liu J, Zhao Z, Xu C, Liu J (2019) Structure, synthesis, and catalytic properties of nanosize cerium-zirconium-based solid solutions in environmental catalysis. Chin J Catal 40:1438–1487

López JM, Gilbank AL, García T, Solsona B, Agouram S, Torrente-Murciano L (2015) The prevalence of surface oxygen vacancies over the mobility of bulk oxygen in nanostructured ceria for the total toluene oxidation. Appl Catal B Environ 174-175:403–412

Lu F (1998) Some heterocyclic polymers and polysiloxanes. J Macromol Sci Polym Rev 38:143–205

Lu Y, Dong W, Ding J, Wang W, Wang A (2019) Hydroxyapatite nanomaterials: synthesis, properties, and functional applications. In: Nanomaterials from clay minerals. Elsevier, Amsterdam/Cambridge, MA, pp 485–536

Maddila S, Maddila SN, Jonnalagadda SB, Lavanya P (2016) Reusable Ce-V loaded alumina catalyst for multicomponent synthesis of substituted pyridines in green media. J Heterocyclic Chem 53:658–664

Maddila SN, Maddila S, van Zyl WE, Jonnalagadda SB (2017a) CeO2/ZrO2 as green catalyst for one-pot synthesis of new pyrano[2,3-c]-pyrazoles. Res Chem Intermed 43:4313–4325

Maddila S, Gangu KK, Maddila SN, Jonnalagadda SB (2017b) A viable and efficacious catalyst, CeO2/HAp, for green synthesis of novel pyrido[2,3-d]pyrimidine derivatives. Res Chem Intermed 44:1397–1409

Maensiri S, Masingboon C, Laokul P, Jareonboon W, Promarak V, Anderson PL, Seraphin S (2007) Egg white synthesis and photoluminescence of Platelike clusters of CeO2Nanoparticles. Cryst Growth Des 7:950–955

Majumdar KC, Chattopadhyay SK (2011) Heterocycles in natural product synthesis. Wiley-VCH, Weinheim

Malik B, Pirzadah TB, Kumar M, Rehman RU (2017) Biosynthesis of nanoparticles and their application in pharmaceutical industry. In: Nanotexhnology, pp 235–252

Maqbool Q (2017) Green-synthesised cerium oxide nanostructures (CeO2-NS) show excellent biocompatibility for phyto-cultures as compared to silver nanostructures (Ag-NS). RSC Adv 7:56575–56585

Melchionna M, Fornasiero P (2014) The role of ceria-based nanostructured materials in energy applications. Mater Today 17:349–357

Moydeen M, Al-Deyab SS, Kumar RS, Idhayadhulla A (2017) Efficient synthesis of novel 3-Phenyl-5-thioxo-3,4,5,6-tetrahydroimidazo[4,5-c]pyrazole-2(1H)-carbothioamide derivatives using a CeO2-MgO catalyst and evaluation of antimicrobial activity. J Heterocyclic Chem 54:3208–3219

Naaz F, Farooq U, Ahmad T (2019) Ceria as an efficient Nanocatalyst for organic transformations. In: Nanocatalysts. IntechOpen, London

Orge CA, Órfão JJM, Pereira MFR, Duarte de Farias AM, Fraga MA (2012) Ceria and cerium-based mixed oxides as ozonation catalysts. Chem Eng J 200-202:499–505

Paier J, Penschke C, Sauer J (2013) Oxygen defects and surface chemistry of ceria: quantum chemical studies compared to experiment. Chem Rev 113:3949–3985

Parashar M, Shukla VK, Singh R (2020) Metal oxides nanoparticles via sol–gel method: a review on synthesis, characterization and applications. J Mater Sci Mater Electron 31:3729–3749

Pokhrel S (2018) Hydroxyapatite: preparation, properties and its biomedical applications. Adv Chem Eng Sci 08:225–240

Polshettiwar V, Luque R, Fihri A, Zhu H, Bouhrara M, Basset JM (2011) Magnetically recoverable nanocatalysts. Chem Rev 111:3036–3075

Pratap SR, Shamshuddin SZM, Thimmaraju N, Shyamsundar M (2020) Cordierite honeycomb monoliths coated with Al(III)/ZrO2 as an efficient and reusable catalyst for the Knoevenagel condensation: a faster kinetics. Arab J Chem 13:2734–2749

Qi G, Li W (2015) NO oxidation to NO2 over manganese-cerium mixed oxides. Catal Today 258:205–213

Qu Y, Gao Y, Lin S, Shi L (2020) Efficient synthesis of 3-methylindole using biomass-derived glycerol and aniline over ZnO and CeO2 modified Ag/SBA-15 catalysts. Mol Catal 493:111038

Rahmat (2010) A review: Mesoporous Santa Barbara Amorphous-15, types, synthesis and its applications towards biorefinery production. Am J Appl Sci 7:1579–1586

Ramachandran M, Subadevi R, Sivakumar M (2019) Role of pH on synthesis and characterization of cerium oxide (CeO2) nano particles by modified co-precipitation method. Vacuum 161:220–224

Ramazani A, Asiabi P, Aghahosseini H, Gouranlou F (2017) Review on the synthesis and functionalization of SiO2 nanoparticles as solid supported catalysts. Curr Org Chem 21:908–922

Rane AV, Kanny K, Abitha VK, Thomas S (2018) Methods for synthesis of nanoparticles and fabrication of nanocomposites. In: Synthesis of inorganic nanomaterials. Wiley, Weinheim, pp 121–139

Rashed MN, Touchy AS, Chaudhari C, Jeon J, Siddiki SMAH, Toyao T, Shimizu K-i (2020) Selective C3-alkenylation of oxindole with aldehydes using heterogeneous CeO2 catalyst. Chin J Catal 41:970–976

Rathod S, Arbad B, Lande M (2010) Preparation, characterization, and catalytic application of a Nanosized Ce1MgxZr1-xO2Solid heterogeneous catalyst for the synthesis of Tetrahydrobenzo[b]pyran derivatives. Chin J Catal 31:631–636

Rico-Pérez V, García-Cortés JM, de Lecea CS-M, Bueno-López A (2013) NOx reduction to N2 with commercial fuel in a real diesel engine exhaust using a dual bed of Pt/beta zeolite and RhOx/ceria monolith catalysts. Chem Eng Sci 104:557–564

Rodriguez JA, Grinter DC, Liu Z, Palomino RM, Senanayake SD (2017) Ceria-based model catalysts: fundamental studies on the importance of the metal-ceria interface in CO oxidation, the water-gas shift, CO2 hydrogenation, and methane and alcohol reforming. Chem Soc Rev 46:1824–1841

Russo N, Mescia D, Fino D, Saracco G, Specchia V (2007) N2O decomposition over perovskite catalysts. Ind Eng Chem Res 46:4226–4231

Saadati-Moshtaghin HR, Zonoz FM (2019) In situ preparation of CeO2 nanoparticles on the MCM-41 with magnetic core as a novel and efficient catalyst for the synthesis of substituted pyran derivatives. Inorg Chem Commun 99:44–51

Sabitha G, Reddy KB, Yadav JS, Shailaja D, Sivudu KS (2005) Ceria/vinylpyridine polymer nanocomposite: an ecofriendly catalyst for the synthesis of 3,4-dihydropyrimidin-2(1H)-ones. Tetrahedron Lett 46:8221–8224

Sabitha G, Reddy N, Prasad M, Yadav J, Sivudu K, Shailaja D (2008) Efficient synthesis of Bis(indolyl)methanes using nano Ceria supported on vinyl pyridine polymer at ambient temperature. Lett Org Chem 5:300–303

Safaei-Ghomi J, Kalhor S, Shahbazi-Alavi H, Asgari-Kheirabadi M (2015a) Three-component synthesis of cyclic β-aminoesters using CeO2 nanoparticles as an efficient and reusable catalyst. Turk J Chem 39:843–849

Safaei-Ghomi J, Heidari-Baghbahadorani E, Shahbazi-Alavi H, Asgari-Kheirabadi M (2015b) A comparative study of the catalytic activity of nanosized oxides in the one-pot synthesis of highly substituted dihydropyridines. RSC Adv 5:18145–18152

Safaei-Ghomi J, Asgari-Keirabadi M, Khojastehbakht-Koopaei B, Shahbazi-Alavi H (2015c) Multicomponent synthesis of C-tethered bispyrazol-5-ols using CeO2 nanoparticles as an efficient and green catalyst. Res Chem Intermed 42:827–837

Safaei-Ghomi J, Shahbazi-Alavi H, Kalhor S (2016) CeO2 nanoparticles: an efficient and robust catalyst for the synthesis of 2-amino-4,6-diarylbenzene-1,3-dicarbonitriles. Monatshefte für Chemie - Chemical Monthly 147:1933–1937

Safari J, Gandomi-Ravandi S (2014a) Application of the ultrasound in the mild synthesis of substituted 2,3-dihydroquinazolin-4(1H)-ones catalyzed by heterogeneous metal–MWCNTs nanocomposites. J Mol Struct 1072:173–178

Safari J, Gandomi-Ravandi S (2014b) Silver decorated multi-walled carbon nanotubes as a heterogeneous catalyst in the sonication of 2-aryl-2,3-dihydroquinazolin-4(1H)-ones. RSC Adv 4:11654–11660

Safari J, Gandomi-Ravandi S (2014c) Titanium dioxide supported on MWCNTs as an eco-friendly catalyst in the synthesis of 3,4-dihydropyrimidin-2-(1H)-ones accelerated under microwave irradiation. New J Chem 38:3514–3521

Samai B, Sarkar S, Chall S, Rakshit S, Bhattacharya SC (2016) Polymer-fabricated synthesis of cerium oxide nanoparticles and applications as a green catalyst towards multicomponent transformation with size-dependent activity studies. CrystEngComm 18:7873–7882

Samantaray S, Pradhan DK, Hota G, Mishra BG (2012) Catalytic application of CeO2–CaO nanocomposite oxide synthesized using amorphous citrate process toward the aqueous phase one pot synthesis of 2-amino-2-chromenes. Chem Eng J 193-194:1–9

Schneider JJ, Naumann M, Schafer C, Brandner A, Hofmann HJ, Claus P (2011) Template-assisted formation of microsized nanocrystalline CeO(2) tubes and their catalytic performance in the carboxylation of methanol. Beilstein J Nanotechnol 2:776–784

Schwarz W, Schossig J, Rossbacher R, Pinkos R, Höke H (2019) Butyrolactone. In: Ullmann's Encyclopedia of industrial chemistry. Weinheim, Wiley, pp 1–7

Shafighi S, Mohammad Shafiee MR, Ghashang M (2018) MgO-CeO2nanocomposite: efficient catalyst for the preparation of 2-aminothiophenes and thieno[2,3-d]pyrimidin-4(3H)-one derivatives. J Sulfur Chem 39:402–413

Sharma K, Borah A, Neog K, Gogoi DP (2016a) CeO2-catalyzed C-H functionalization ofN-Aryltetrahydroisoquinolines: an aerobic cross-Dehydrogenative coupling reaction between two sp3C-H bonds. Chem Select 1:4620–4623

Sharma RK, Dutta S, Sharma S, Zboril R, Varma RS, Gawande MB (2016b) Fe3O4(iron oxide)-supported nanocatalysts: synthesis, characterization and applications in coupling reactions. Green Chem 18:3184–3209

Sharma K, Das B, Gogoi P (2018) Synthesis of pyrrolo[3,4-c]quinoline-1,3-diones: a sequential oxidative annulation followed by dehydrogenation and N-demethylation strategy. New J Chem 42:18894–18905

Shelkar R, Sarode S, Nagarkar J (2013) Nano ceria catalyzed synthesis of substituted benzimidazole, benzothiazole, and benzoxazole in aqueous media. Tetrahedron Lett 54:6986–6990

Shelkar RS, Balsane KE, Nagarkar JM (2015) Magnetically separable nano CeO2: a highly efficient catalyst for ligand free direct C–H arylation of heterocycles. Tetrahedron Lett 56:693–699

Shen M, Wang J, Shang J, An Y, Wang J, Wang W (2009) Modification Ceria-Zirconia mixed oxides by doping Sr using the reversed microemulsion for improved Pd-only three-way catalytic performance. J Phys Chem C 113:1543–1551

Shi Z-L, Du C, Yao S-H (2011) Preparation and photocatalytic activity of cerium doped anatase titanium dioxide coated magnetite composite. J Taiwan Inst Chem Eng 42:652–657

Shimura S, Miura H, Wada K, Hosokawa S, Yamazoe S, Inoue M (2011) Ceria-supported ruthenium catalysts for the synthesis of indole via dehydrogenative N-heterocyclization. Cat Sci Technol 1:1340

Shrestha R, Sharma K, Lee YR, Wee YJ (2016) Cerium oxide-catalyzed multicomponent condensation approach to spirooxindoles in water. Mol Divers 20:847–858

Sifontes AB, Gonzalez G, Ochoa JL, Tovar LM, Zoltan T, Cañizales E (2011) Chitosan as template for the synthesis of ceria nanoparticles. Mater Res Bull 46:1794–1799

Soni B, Biswas S (2013) Ceria nanoparticles synthesized by a polymer precursor method. Int J Modern Phys Conf Ser 22:169–172

Spezzati G, Su Y, Hofmann JP, Benavidez AD, DeLaRiva AT, McCabe J, Datye AK, Hensen EJM (2017) Atomically dispersed Pd–O species on CeO2(111) as highly active sites for low-temperature CO oxidation. ACS Catal 7:6887–6891

Sultana SSP, Kishore DHV, Kuniyil M, Khan M, Alwarthan A, Prasad KRS, Labis JP, Adil SF (2015) Ceria doped mixed metal oxide nanoparticles as oxidation catalysts: synthesis and their characterization. Arab J Chem 8:766–770

Sun W, Liu D-Y, Zhu H-Y, Shi L, Sun Q (2010) A new efficient approach to 3-methylindole: vapor-phase synthesis from aniline and glycerol over Cu-based catalyst. Catal Commun 12:147–150

Sun C, Li H, Chen L (2012) Nanostructured ceria-based materials: synthesis, properties, and applications. Energy Environ Sci 5:8475

Sungkono IE, Kameyama H, Koya T (1997) Development of catalytic combustion technology of VOC materials by anodic oxidation catalyst. Appl Surf Sci 121-122:425–428

Suresh L, Vijay Kumar PS, Vinodkumar T, Chandramouli GVP (2016) Heterogeneous recyclable nano-CeO2 catalyst: efficient and eco-friendly synthesis of novel fused triazolo and tetrazolo pyrimidine derivatives in aqueous medium. RSC Adv 6:68788–68797

Suvetha Rani J (2020) Green synthesis and characterization of Ceria nanoparticles using Ricinus communis leaf extract. Int J Sci Res Publ 10:9743

Tamura M, Noro K, Honda M, Nakagawa Y, Tomishige K (2013a) Highly efficient synthesis of cyclic ureas from CO2 and diamines by a pure CeO2 catalyst using a 2-propanol solvent. Green Chem 15:1567

Tamura M, Honda M, Noro K, Nakagawa Y, Tomishige K (2013b) Heterogeneous CeO2-catalyzed selective synthesis of cyclic carbamates from CO2 and aminoalcohols in acetonitrile solvent. J Catal 305:191–203

Tamura M, Ito K, Nakagawa Y, Tomishige K (2016a) CeO2-catalyzed direct synthesis of dialkylureas from CO2 and amines. J Catal 343:75–85

Tamura M, Ito K, Honda M, Nakagawa Y, Sugimoto H, Tomishige K (2016b) Direct copolymerization of CO2 and diols. Sci Rep 6:24038
Taylor AP, Robinson RP, Fobian YM, Blakemore DC, Jones LH, Fadeyi O (2016) Modern advances in heterocyclic chemistry in drug discovery. Org Biomol Chem 14:6611–6637
Terribile D, Trovarelli A, Llorca J, de Leitenburg C, Dolcetti G (1998) The synthesis and characterization of mesoporous high-surface area ceria prepared using a hybrid organic/inorganic route. J Catal 178:299–308
Thakur N, Manna P, Das J (2019) Synthesis and biomedical applications of nanoceria, a redox active nanoparticle. J Nanobiotechnol 17:84
Thovhogi N, Diallo A, Gurib-Fakim A, Maaza M (2015) Nanoparticles green synthesis by Hibiscus Sabdariffa flower extract: Main physical properties. J Alloys Compd 647:392–396
Tillirou AA, Theocharis CR (2008) Synthesis and characterization of mesoporous cerium oxide prepared using an organic base and a templating agent. Adsorp Sci Technol 26:687–692
Tomishige K, Yasuda H, Yoshida Y, Nurunnabi M, Li B, Kunimori K (2004) Catalytic performance and properties of ceria based catalysts for cyclic carbonate synthesis from glycol and carbon dioxide. Green Chem 6:206
Tomishige K, Tamura M, Nakagawa Y (2019) CO2 conversion with alcohols and amines into carbonates, ureas, and carbamates over CeO2 catalyst in the presence and absence of 2-Cyanopyridine. Chem Rec 19:1354–1379
Tomishige K, Gu Y, Nakagawa Y, Tamura M (2020) Reaction of CO2 with alcohols to linear-, cyclic-, and poly-carbonates using CeO2-based catalysts. Front Energy Res 8:117
Tsai M-S (2004) Powder synthesis of nano grade cerium oxide via homogenous precipitation and its polishing performance. Mater Sci Eng B 110:132–134
Vadivel P, Ramesh R, Lalitha A (2013) Ceric ion loaded MCM-41 catalyzed synthesis of substituted mono- and Bis-dihydropyrimidin-2(1H)-ones. J Catal 2013:1–8
Venkatesh SZM, Shamshuddin NM (2015) Mubarak, effective synthesis of quinoxalines over ceria based solid acids coated on honeycomb monoliths. Indian J Chem 54A:843–850
Vijay Kumar PS, Suresh L, Vinodkumar T, Chandramouli GVP (2016) Eu2O3 modified CeO2 nanoparticles as a heterogeneous catalyst for an efficient green multicomponent synthesis of novel phenyldiazenyl-acridinedione-carboxylic acid derivatives in aqueous medium. RSC Adv 6:91133–91140
Vita A, Italiano C, Ashraf MA, Pino L, Specchia S (2018a) Syngas production by steam and oxy-steam reforming of biogas on monolith-supported CeO 2 -based catalysts. Int J Hydrog Energy 43:11731–11744
Vita A, Italiano C, Pino L, Frontera P, Ferraro M, Antonucci V (2018b) Activity and stability of powder and monolith-coated Ni/GDC catalysts for CO2 methanation. Appl Catal B Environ 226:384–395
Vitaku E, Smith DT, Njardarson JT (2014) Analysis of the structural diversity, substitution patterns, and frequency of nitrogen heterocycles among U.S. FDA approved pharmaceuticals. J Med Chem 57:10257–10274
Vivier L, Duprez D (2010) Ceria-based solid catalysts for organic chemistry. ChemSusChem 3:654–678
Walsh CT (2015) Nature loves nitrogen heterocycles. Tetrahedron Lett 56:3075–3081
Wang S, Wang Z, Zha Z (2009) Metal nanoparticles or metal oxide nanoparticles, an efficient and promising family of novel heterogeneous catalysts in organic synthesis. Dalton Trans 2009:9363–9373
Wang Y, Ge W, Fang Y, Ren X, Cao S, Liu G, Li M, Xu J, Wan Y, Han X, Wu H (2016) Porous CeO2 nanorod-catalyzed synthesis of poly-substituted imino-pyrrolidine-thiones. Res Chem Intermed 43:631–640
Wang Y, Arandiyan H, Scott J, Bagheri A, Dai H, Amal R (2017) Recent advances in ordered meso/macroporous metal oxides for heterogeneous catalysis: a review. J Mater Chem A 5:8825–8846

Xu P, Yu R, Ren H, Zong L, Chen J, Xing X (2014) Hierarchical nanoscale multi-shell Au/CeO2 hollow spheres. Chem Sci 5:4221–4226

Xu B, Qi F, Sun D, Chen Z, Robert D (2016) Cerium doped red mud catalytic ozonation for bezafibrate degradation in wastewater: efficiency, intermediates, and toxicity. Chemosphere 146:22–31

Yan B, Zhang Y, Chen G, Shan R, Ma W, Liu C (2016) The utilization of hydroxyapatite-supported CaO-CeO2 catalyst for biodiesel production. Energy Convers Manag 130:156–164

Yin P, Shreeve JNM (2017) Nitrogen-rich azoles as high density energy materials. In: Advances in heterocyclic chemistry, vol 121, pp 89–131

Yu T, Joo J, Park YI, Hyeon T (2005) Large-scale nonhydrolytic sol-gel synthesis of uniform-sized ceria nanocrystals with spherical, wire, and tadpole shapes. Angew Chem Int Ed Engl 44:7411–7414

Yu B, Zhang H, Zhao Y, Chen S, Xu J, Hao L, Liu Z (2013) DBU-based ionic-liquid-catalyzed carbonylation of o-Phenylenediamines with CO2 to 2-Benzimidazolones under solvent-free conditions. ACS Catal 3:2076–2082

Zamani A, Marjani AP, Alimoradlu K (2018) Walnut Shell-templated ceria nanoparticles: green synthesis, characterization and catalytic application. Int J Nanosci 17:1850008

Zarnegar Z, Safari J, Kafroudi ZM (2015) Co3O4–CNT nanocomposites: a powerful, reusable, and stable catalyst for sonochemical synthesis of polyhydroquinolines. New J Chem 39:1445–1451

Zhang QL, Yang ZM, Ding BJ (2009) Synthesis of cerium oxide nanoparticles by the precipitation method. Mater Sci Forum 610-613:233–238

Zhang D, Du X, Shi L, Gao R (2012) Shape-controlled synthesis and catalytic application of ceria nanomaterials. Dalton Trans 41:14455–14475

Zhang Y, Chen C, Gong W, Song J, Zhang H, Zhang Y, Wang G, Zhao H (2017) Self-assembled Pd/CeO 2 catalysts by a facile redox approach for high-efficiency hydrogenation of levulinic acid into gamma-valerolactone. Catal Commun 93:10–14

Zhang X, Song Y, Guan F, Zhou Y, Lv H, Wang G, Bao X (2018) Enhancing electrocatalytic CO2 reduction in solid oxide electrolysis cell with Ce0.9Mn0.1O2−δ nanoparticles-modified LSCM-GDC cathode. J Catal 359:8–16

Zhao X, Chaudhry ST, Mei J (2017) Heterocyclic building blocks for organic semiconductors. In: Advances in heterocyclic chemistry, vol 121, pp 133–171